Approved for public release; distribution is unlimited

Factors Influencing the Microstructure and Mechanical Properties of Ultra Low Carbon Bainitic 100 Tungsten Inert Gas Multipass Weldments

by

Eugene Paul McDonald
Lieutenant, United States Navy
B.S., University Of Utah, 1985

Submitted in partial fulfillment of the
requirements for the degree of

MASTER OF SCIENCE IN MECHANICAL ENGINEERING

from the

NAVAL POSTGRADUATE SCHOOL
September, 1992

RITY CLASSIFICATION OF THIS PAGE

REPORT DOCUMENTATION PAGE

REPORT SECURITY CLASSIFICATION: UNCLASSIFIED	1b. RESTRICTIVE MARKINGS
SECURITY CLASSIFICATION AUTHORITY	3. DISTRIBUTION/AVAILABILITY OF REPORT: Approved for public release; distribution is unlimited
DECLASSIFICATION/DOWNGRADING SCHEDULE	
ERFORMING ORGANIZATION REPORT NUMBER(S)	5. MONITORING ORGANIZATION REPORT NUMBER(S)
NAME OF PERFORMING ORGANIZATION: ech. Engineering Dept. val Postgraduate School; 6b. OFFICE SYMBOL (if applicable): ME	7a. NAME OF MONITORING ORGANIZATION: Naval Postgraduate School
ADDRESS (City, State, and ZIP Code): nterey, CA 93943-5000	7b. ADDRESS (City, State, and ZIP Code): Monterey, CA 93943-5000
NAME OF FUNDING/SPONSORING ORGANIZATION: vid Taylor Research Center; 8b. OFFICE SYMBOL (if applicable): Code 2814	9. PROCUREMENT INSTRUMENT IDENTIFICATION NUMBER
ADDRESS (City, State, and ZIP Code): napolis, MD 21402	10. SOURCE OF FUNDING NUMBERS: PROGRAM ELEMENT NO. / PROJECT NO. / TASK NO. / WORK UNIT ACCESSION

TITLE (Include Security Classification)
ors Influencing the Microstructure and Mechanical Properties of Ultra Low Carbon Bainitic 100 Tungsten Inert Gas Multipass Weldments

PERSONAL AUTHOR(S)
Eugene Paul McDonald

TYPE OF REPORT	13b. TIME COVERED	14. DATE OF REPORT (Year, Month, Day)	15. PAGE COUNT
ster's Thesis	FROM 04/92 TO: 09/92	1992, SEPTEMBER	65

SUPPLEMENTARY NOTATION: The views expressed in this thesis are those of the author and do not reflect the officia policy or position of the Department of Defense or the United States Government.

COSATI CODES			18. SUBJECT TERMS (Continue on reverse if necessary and identify by block number)
IELD	GROUP	SUB-GROUP	Ultra Low Carbon Bainitic Steel

ABSTRACT (Continue on reverse if necessary and identify by block number)

The U.S. Navy has maintained a continuous research, development and certification program in HSLA and ULCB steels with the int omeday totally replacing the HY steels now used in ship construction. A major advantage in using HSLA and ULCB steels is th ease in weldability over the HY steels which now require large amounts of preheating to prevent crack formation in the heat affec e. Up until the present day, however, low carbon HSLA and ULCB steels have not been used with a dedicated low carbon weld wire present work an attempt was made to correlate the mechanical properties (tensile strength, yield strength and Charpy impact energ mical composition and microstructure of a series of autogenous multirun TIG welds on ULCB steels. It was found that good combinati veld strength and toughness could be achieved with appropriate choice of weld metal chemistry and TIG welding power, but that th a ceiling of about 2.0wt.% molybdenum which could be tolerated before weld metal embrittlement became evident.

DISTRIBUTION/AVAILABILITY OF ABSTRACT: UNCLASSIFIED/UNLIMITED ☐ SAME AS RPT. ☐ DTIC USERS	21. ABSTRACT SECURITY CLASSIFICATION: UNCLASSIFIED
NAME OF RESPONSIBLE INDIVIDUAL: n G. Fox	22b. TELEPHONE (Include Area Code): (408) 646-2142 / 22c. OFFICE SYMBOL: ME/Fx

ORM 1473, 84 MAR — 83 APR edition may be used until exhausted. All other editions are obsolete — SECURITY CLASSIFICATION OF THIS PAGE: UNCLASSIFIED

ABSTRACT

The U.S. Navy has maintained a continuous research, development and certification program in HSLA and ULCB steels with the intent of someday totally replacing the HY steels now used in ship construction. A major advantage in using HSLA and ULCB steels is their increase in weldability over the HY steels which now require large amounts of preheating to prevent crack formation in the heat affected zone. Up until the present day, however, low carbon HSLA and ULCB steels have not been used with a dedicated low carbon weld wire. In the present work an attempt was made to correlate the mechanical properties (tensile strength, yield strength and Charpy impact energy), chemical composition and microstructure of a series of autogenous multirun TIG welds on ULCB steels. It was found that good combinations of weld strength and toughness could be achieved with appropriate choice of weld metal chemistry and TIG welding power, but that there was a ceiling of about 2.0wt.% molybdenum which could be tolerated before weld metal embrittlement became evident.

Table of Contents

LIST OF FIGURES

ACKNOWLEDGEMENTS

I would like to thank Dr. Alan G. Fox for his invaluable knowledge, guidance and motivation over the course of this study. His skill in operating the scanning electron microscope proved crucial to the successful completion of this project. Thank you Dr. Michael G. Vassilaros of the David Taylor Research Center for providing the Ultra Low Carbon Bainitic steel weldment samples, data and advice. And last but not least my lovely wife Kyoko for her months of patient support in helping me accomplish this goal.

I. INTRODUCTION

The object of this thesis is to investigate the influences of different alloying elements and developed microstructures upon the strength and toughnesses obtained in Ultra Low Carbon Bainitic (ULCB) 100 steel multi pass TIG weldments. ULCB steel is a relatively new family of steels which has been found to be ideal for the development of stronger and tougher weld metals.

The U.S. Navy has maintained a continuous research, development and certification program in HSLA steels over the past decade in order to replace the use of HY steels in hull construction. Tougher and stronger steels are required to build submarines capable of greater depths and speeds. The greater strengths and toughnesses of ULCB and HSLA steels will support higher pressures allowing greater operating depths and will reduce their weight corresponding to greater speeds. These steels also substantially reduce the cost of hull fabrication and required construction times by nearly eliminating the stringent welding controls necessary in HY series hull construction. Many hours of preheating HY series steels is required to prevent Hydrogen-induced cold cracking in the weld metal and the HAZ (Irving, 1987, p.34). The use of ULCB weld wire upon HSLA-130 low carbon base metal reduces the amount of carbon diffusion into the weld metal and correspondingly increases the fracture toughness of the weld.

This study investigated the microstructure, fracture surfaces, inclusions, and data obtained from various mechanical properties tests in order to determine the mechanisms responsible for the strength, toughness and possible embrittlement of autogenous ULCB TIG weldments.

II. BACKGROUND

A. HIGH YIELD AND HIGH STRENGTH LOW ALLOY STEELS

High yield (HY) steels are produced using typical quench and temper methods in order to attain strengths greater than 690MPa (100Ksi). Carbon and other alloying elements such as Mn, Mo, Ni and Cr are added to increase the strength and hardenability of the steel. However, substantial limitations on the plate thickness, interpass temperature and heat input exist when welding HY steels. The maximum heat input is limited due to the high cooling rates required in the weld in order to maintain the desired high strengths. In addition long hours of preheating HY steels are required in order to reduce the welds susceptibility to hydrogen induced cold cracking (HIC). Preheating is a costly and time consuming procedure which has inspired research into alternative steels.

The U.S. Navy has sponsored extensive research into the development of High Strength Low Alloy (HSLA) steels with the intent of their replacing the HY steels. Hull fabrication costs have been reduced substantially through the use of HSLA steels due mainly to the near elimination of the preheating requirements and their low susceptibility to HIC. The low carbon HSLA steels achieve their high strengths through copper precipitation strengthening and non-recrystallization controlled rolling thermomechanical processing. HSLA-80 steel was certified in 1980 and is currently the primary hull construction material for the CG-47, DDG-51, CVN 68 AND LHD-1 class ships (Gudas, 1989, p.3). HSLA-100 steel was certified in 1989 and is being used in the construction of the John C. Stennis CVN 74. The higher strength HSLA-100 steel is attained through increased copper alloying resulting in more precipitation strengthening along with higher amounts of Mn, Mo, Ni, and Cr to improve its hardenability (Czyryca, Link, 1988, p.3). The continued development of HY and HSLA steels has resulted in carbon contents being lowered to below 0.10

weight percent carbon. The Graville diagram in Figure 2.1 illustrates that low carbon content steels are more easily weldable than the HY steels over the whole range of carbon equivalent values (CEV). The CEV is a measure of a metal's ability to resist hydrogen induced cracking. The HY steels because of their higher carbon and alloying contents are more susceptible to hydrogen induced cold cracking whereas the low carbon HSLA and ULCB steels in Zone I are easily weldable regardless of their CEV.

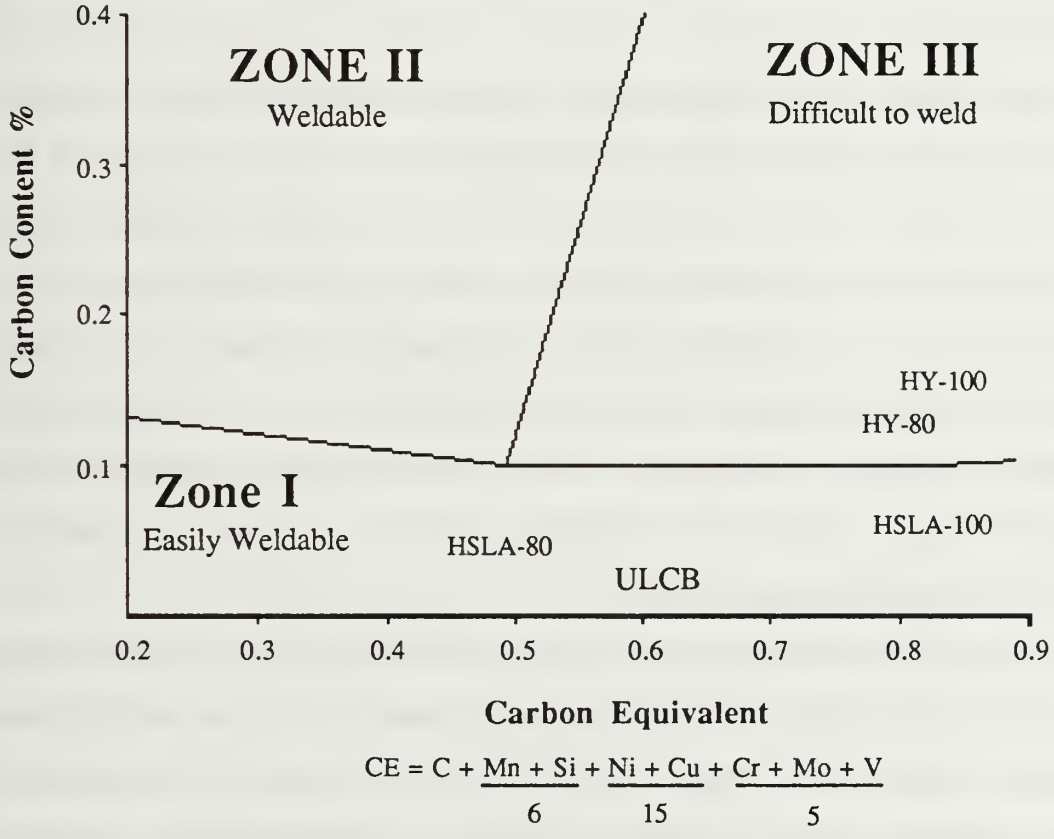

Figure 2.1 Graville Diagram
(Blicharski et al, 1989, p.318)

B. ULTRA LOW CARBON BAINITIC STEEL

Ultra Low Carbon Bainitic steels have been developed as an alternative to the HY and HSLA steels. Yield strengths greater than 690MPa (100Ksi) are obtained in ULCB steels while maintaining a high resistance to both brittle and ductile fracture. This is accomplished through strict control of alloying contents and through the use of advanced thermomechanical processing techniques. The high strengths attained are attributed to solid solution strengthening and induced dislocation substructures (Blicharski et al., 1988, p.319). The Navy Surface Warfare Center, Annapolis Detachment has recently shown that the toughness of 0.02 - 0.04 percent ULCB steels is closely related to the content of inclusions and grain refinement (Gudas, 1989, P.8).

The strengths and toughnesses of welds are highly dependent upon the microstructures created during the welding process. Of primary interest is the differing forms of bainite that result in the weld. At relatively lower transformation temperatures the precipitation of carbon out of the prior austenite grains results in the formation of carbides into discrete particles surrounded by a ferrite matrix. This microconstituent, or arrangement of ferrite and cementite, is called Bainite. Bainitic microstructures form in conjunction with a mix of martensite, retained austenite, pearlite, acicular ferrite and Widmanstätten ferrite. It is thus often difficult to identify the differing bainitic forms.

The bainitic microconstituent is separated into Upper and Lower categories and are distinguished by the size and shape of their laths as well as the size and distribution of carbides. Upper Bainite forms at relatively high transformation temperatures above 350 ° C (Pickering, 1978, p. 110). Precipitating carbon from austenite grains reduces the metals free energy by forming into more rounded, discrete carbide particles. This form minimizes the ferrite-cementite interface area

and thus reduces the associated surface energies. At this relatively low transformation temperature diffusion of particles is very difficult and the migration of elements takes place over small distances. Carbon precipitates out of the austenite in front of growing ferrite laths forming carbides between the ferrite laths.

A decrease in the transformation temperature produces a simultaneous increase in the dislocation density of the microstructure. Dislocation density is additionally strongly controlled by the alloying contents and the thermomechanical processing. Lower Bainite forms at lower transformation temperatures typically around 350° Celsius. The resistance to carbon diffusion at these temperatures is even greater and prevents carbon from reaching lath boundaries and thus carbides precipitate within the ferrite laths (Pickering, 1978, pp. 110-111). Lower bainitc structures are unable to form in ULCB steel, however, due to the high martensite start temperatures above 350 ° Celsius which are characteristic of steels containing less than 0.5 percent Carbon (Samuels, 1980, p.302).

The strength of bainitic steels is directly associated with dislocation density, solid solution strengthening, bainitic lath formation, and the distribution, composition and size of carbides. Dislocations act as impediments to the movement of dislocations. Increasing dislocation density strengthens the steel by resisting the movement of dislocations and associated slip. The number of dislocations is a function of the alloying content and thermomechanical processing of the steel and is known to increase with decreasing transformation temperature. The formation of carbides between laths in upper bainite may provide strengthening by impeding their ability to slip. Bainite microstructures have been shown to have a higher dislocation density than either polygonal or Widmanstätten ferrites. In addition there is experimental evidence which indicates carbon atoms bound to dislocations exist in bainitic ferrite and make a significant contribution to strength.

The strength and toughnesses obtained from bainitic structures has been connected in various studies with lath and colony dimensions. Interlocking acicular ferrite microstructures in weld metals is widely acknowledged to improve toughness. The acicular ferrite structure increases the number of interfaces which halt and redirect the propagation of cracks. Forcing a crack to take a more arduous course results in increasing the toughness of the steel. Figure 2.2 graphically illustrates the crack propagation behavior in three different microstructures. Crack propagation in lath martensite for example is relatively easy due to the like crystallographic orientation of the laths within each subgrain colony. Much of the research conducted to date on strengthening ULCB steels has been concerned with maximizing the formation of acicular ferrite (Matlock, Edwards, 1985, pp.8-9).

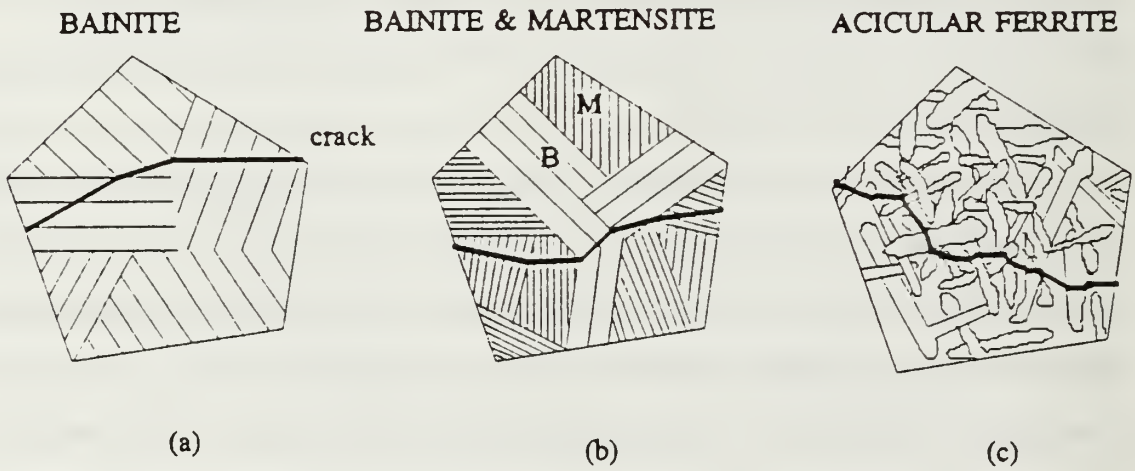

Figure 2.2 Dependence of crack propagation upon microstructure.
Crack deflection due to:

(a) colony boundaries in bainite
(b) subdivided bainite in prior austenite grains
(c) lath boundaries in acicular ferrite

Transformation temperatures associated with the formation of acicular ferrite are typically lower than those of upper bainite for similarly alloyed steels. Indeed precipitation of carbides in ULCB steels is severely reduced due to their low carbon content thus the upper bainite morphology can be considered to be a bainitic ferrite. These and other similarities lend credence to Edmonds' and Cochrane's proposition that acicular ferrite is another form of bainite. (Edmonds, Cochrane, 1990, p.1536).

Significant reductions in weld metal toughness have been attributed to formations of large colonies of upper bainite caused by low oxygen content and large alloying additions. A low oxygen content prevents the formation of inclusions on which acicular ferrite nucleates thus resulting in the formation of a more brittle upper bainite. Evidence supports that primary nucleation on weld metal inclusions as well as secondary nucleation is the mechanism for the formation of acicular ferrite (Edmonds, Cochrane, 1990, p.1536).

Reducing the carbon equivalent value (CEV) in ultra low carbon steel can improve its weldability. Molybdenum and Nickel are added to ULCB steels in larger quantities (2-5wt%) to lower the transformation temperatures. This technique thus exploits austenite transformation strengthening (Edmond, Cochrane, 1990, p.1534).

ULCB weld metal microstructures depend upon the prior austenite grain size and composition as well upon the austenites characteristics of transformation. Grain boundary ferrite forms at high transformation temperatures upon the prior austenite grain boundaries. At lower temperatures diffusion is more restricted resulting in the formation of proeutectic sideplate ferrite. This ferrite finds room to grow into the grain along crystallographically preferred directions. Widmanstätten ferrite forms as the transformation temperature is lowered. The ferrite sideplates associated with Widmanstätten ferrite grow long and needlelike into the grain. At lower transformation temperatures acicular ferrite forms. Most acicular ferrite develops within the prior austenite grains and have large angles between adjacent laths. As

the transformation is further reduced Bainite and Martensite are produced in succession. The solidified microstructure is substantially controlled by the cooling rate. The amount of time required to cool the steel from 800° to 500° C is widely accepted as the basis for the thermal conditions under which the austenite to ferrite transformation occurs. Typically, rapid cooling time (<5s) are associated with martensitic and/or bainitic microstructures whereas moderate cooling times (5-100s) promote acicular ferrite, ferrite sideplates and/or pearlite (Grong, Matlock, 1986, p.37). The relative effects of different cooling rates on weld metal microstructural transformations is displayed in Figure 2.3. The chemical composition of ULCB steel controls the bainite start temperature and the bainite start temperature has an inverse linear relationship with the strength of bainitic steels. This is shown in Figure 2.4 (Blicharski et al., 1988, p.326).

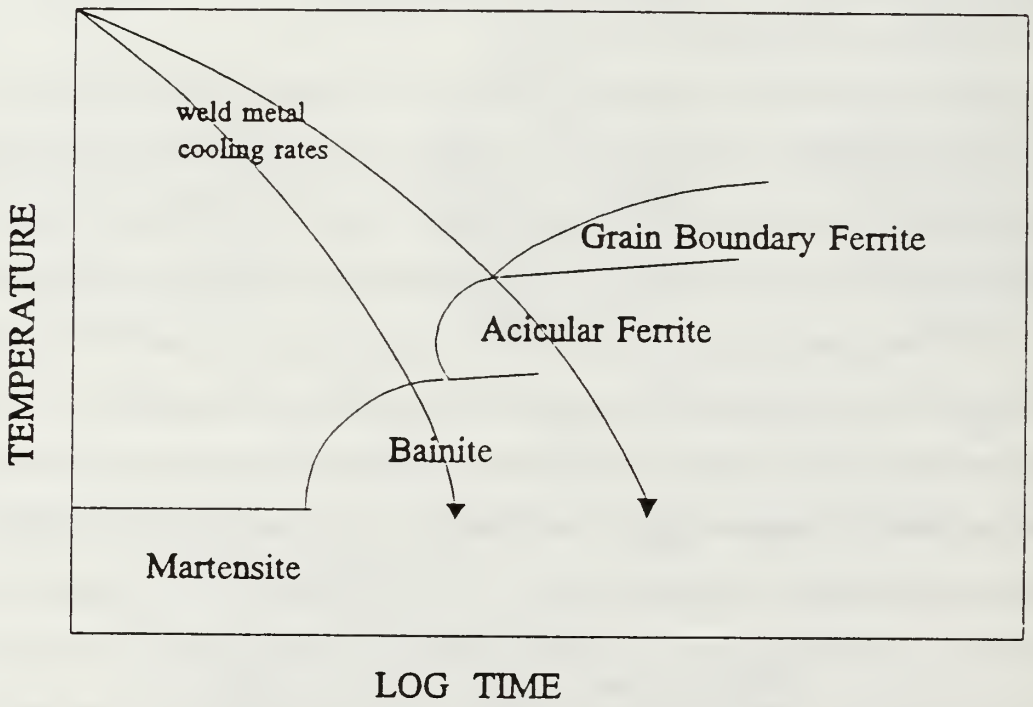

Figure 2.3 Continuous Cooling Transformation Curves.
(McHale, P.F., 1991, p.12)

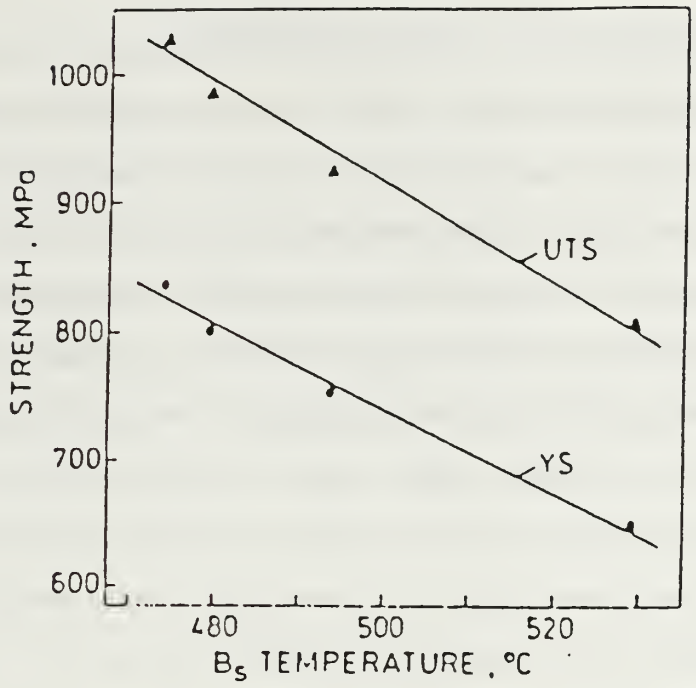

Figure 2.4 Bainite Start Temp. influence on strength
(Blicharski et al., 1988, p.324).

Many factors influence the resulting strength and toughness obtained from ULCB weldments. The alloying mix, heat input rate, cooling rate, weld pool geometry, welding methods, and the presence of nonmetallic inclusions all determine the final microstructure. The aim of welding research is to find the best combination of these factors in order to produce a weld metal with maximum strength and toughness.

C. TUNGSTEN INERT GAS (TIG) WELDING

Tungsten inert gas welding uses a non-consumable tungsten electrode to transfer an arc to the base metal in order to produce the weld. As seen in Figure 2.5 inert gases such as Argon and Helium shield the weld zone to prevent oxygen and other contaminants in the surrounding atmosphere from diffusing into the weld metal and forming oxides and other uncontrollable and detrimental inclusions. The shield gas in conjunction with a short and stable arc make TIG welding the cleanest arc welding process available. Argon is more often used instead of helium in TIG welding because it is easier to ionize and thus arc initiation is more readily attained. Argon also allows a lower voltage drop across the arc and because it is heavier than helium it provides a better shielding effect (Kou, 1987, p.11).

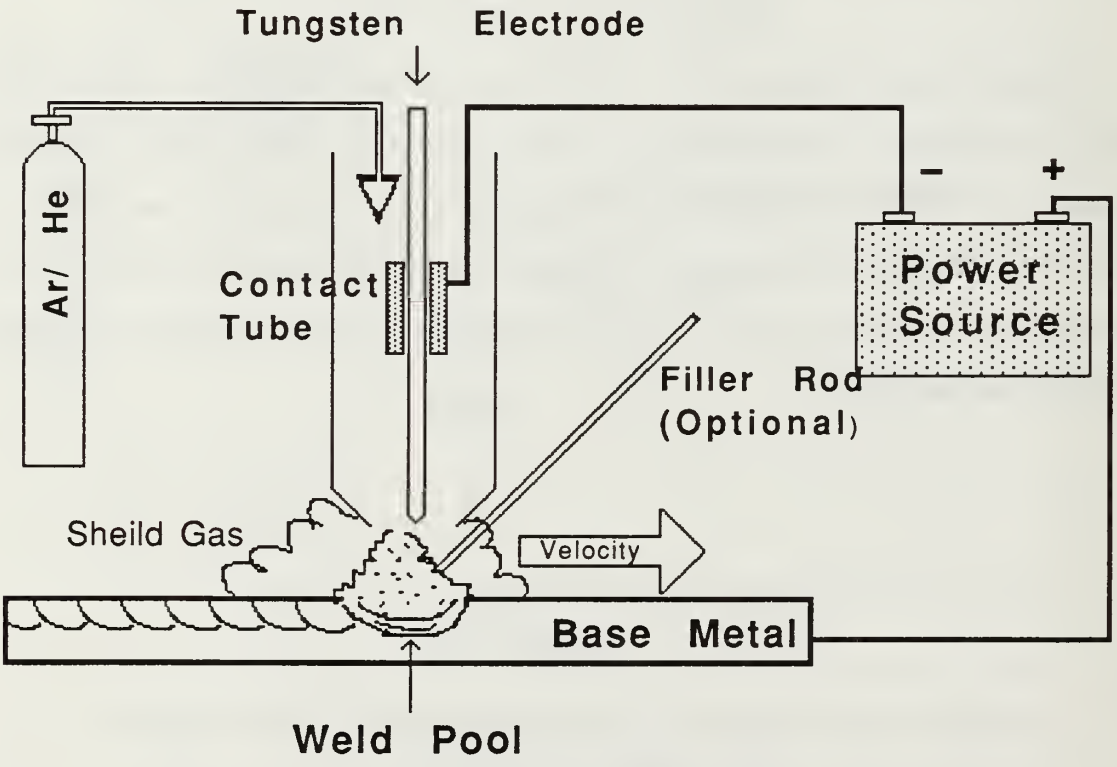

Figure 2.5 Tungsten Inert Gas (TIG) Welding Process

Two electrical configurations are used in TIG welding. Direct-current straight polarity (DCSP) and direct-current reverse polarity (DCRP). In DCSP the electrode is connected to the negative terminal of the power source and the heating effect is induced on the base metal resulting in narrow, deep welds. These type welds are often the most desirable. In DCRP the heating effect is created in the tungsten electrode which requires water-cooled, larger diameter electrodes and produces undesirable shallow welds which are usually undesirable (Kou, 1987, p.10).

D. INFLUENCE OF ALLOYING ELEMENTS ON WELD METAL STRENGTH AND TOUGHNESS

Alloying elements in the weld metal come from either the filler wire or through dilution from the base metal. Most alloying elements such as C, Mn, Mo, Ni, and Cr increase hardenability. The direct effect of each of the alloying elements is often hard to determine however due to the complexity of their interaction during microstructural development. An optimum combination of elements is thus sought to control the microstructure of the weld metal to maximize strength and toughness. Figure 2.6 gives a relative indication of the hardening effect of different elements.

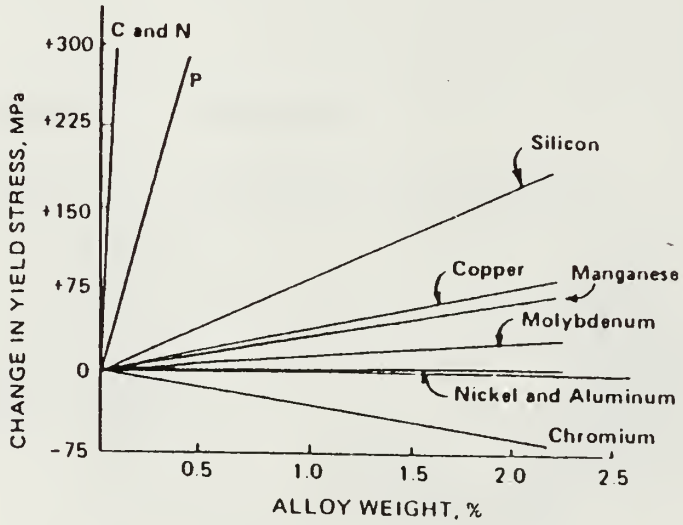

Figure 2.6 Hardening effect of elements in steel.

(Pickering, 1978, p.11)

1. Carbon

Carbon is a solid solution strengthener and greatly improves steel hardness. Increasing the amount of carbon results in higher levels of carbides and produces grain size refinement. The primary strengthening mechanism attributed to carbon is derived from the hard carbides they form (Askeland, 1989, p.336). Although beneficial as strengtheners these same carbides can also act quite detrimentally as crack initiation sites. To minimize hydrogen induced cold cracking fracture attributed to brittle material formation in the heat affected zone carbon contents must be kept low. (Easterling, 1989, p185) Studies of gas shielded weld deposits have found that increasing carbon content from 0.1% to 0.2% decreases the impact toughness. (Abson, Pargeter, 1986, p.153) Thus an increase in toughness can be obtained by reducing the level of carbon below 0.1%.

2. Manganese

Manganese is used as a solid solution strengthener in weld metals and also has a slight deoxidizing effect. Manganese is beneficial in increasing the acicular ferrite while retarding the growth of grain boundary ferrite (Abson, Pargeter, 1986, p.145). Improved toughnesses have been obtained through a refinement of the microstructure attributed to increasing levels of manganese (Abson, Pargeter, 1986, pp.154-159). Manganese also acts as an austenite stabilizer and lowers the temperature of austenite transformation to ferrite.

3. Molybdenum

Molybdenum has a solid solution strengthening effect but is also used to increase toughness and can improve the quantity of acicular ferrite formation (Abson, Pargeter, 1986, p.170).

4. Chromium

Chromium is used as a solid solution strengthener and also forms into hard carbides. In the quenched and tempered HY steels it serves as a hardenability agent. (Hertzberg, 1989, p.376) The effect that both chromium and molybdenum play is not wholly understood however it is believed that the resulting Cr and Mo carbides may slow the formation of proeutectoid ferrite in the prior austenite grain boundaries by either pinning or dragging effects. (Grong, Matlock, 1986, p.38)

5. Nickel

Nickel is used to lower the transformation temperature of austenite to ferrite and also improves toughness by refining the acicular ferrite. Studies indicate that it serves to stabilize austenite as well. (Abson, Pargeter, 1986, p.170).

6. Titanium

Titanium precipitates from nitrides and carbides may act as nucleation sites for acicular ferrite. Inclusions found to contain titanium have been found to be very effective in nucleating intragranular acicular ferrite (Kiessling, 1989, p.105).

7. Aluminum

Aluminum serves as a very effective deoxidizer. The formation of aluminum nitrides which pin grain boundaries and slow grain growth also serve to refine the grain structure in the weld metal and thus increase toughness.

E. SCOPE OF PRESENT WORK

Ultra Low Carbon Bainitic steels are of high interest to the United States Navy because high strengths and toughnesses can be obtained with the added benefit of high weldability. The present immediate interest is in the development of ULCB weld wire to be used with HSLA and ULCB steels in the construction of U.S. naval vessels. Twenty two ULCB ingots of differing compositions (Table 3.1) were cast using the same thermomechanical processing to increase strength and toughness. An average of 12 specimens of each ingot were tested for varying mechanical properties then sent to the Naval Postgraduate School for further research. The range of yield strengths and toughnesses obtained were quite scattered as shown in Figure 4.1 and Figure 4.2 on page 21. This yielded no immediate solution to obtaining a sample with optimum properties. A study of the effects of the different weld powers and differing compositions was thus conducted in order to determine what factors were leading to embrittlement of the metal and which factors enhanced its strength and toughness.

III. EXPERIMENTAL PROCEDURE

A. WELDMENT SAMPLES

The Naval Surface Warfare Center, Annapolis Detachment supplied Ultra low Carbon Bainitic (ULCB) steel weldment samples. The steel for these was in the form of plates of 1.25 in thickness which had been cut out of the center of the ULCB ingots. Steel filler wire was cut from other regions of the same ingots. Charpy samples were cut in a transverse direction to the weld beads The chemical composition of each of the ULCB samples is listed in Figure 3.1 below.

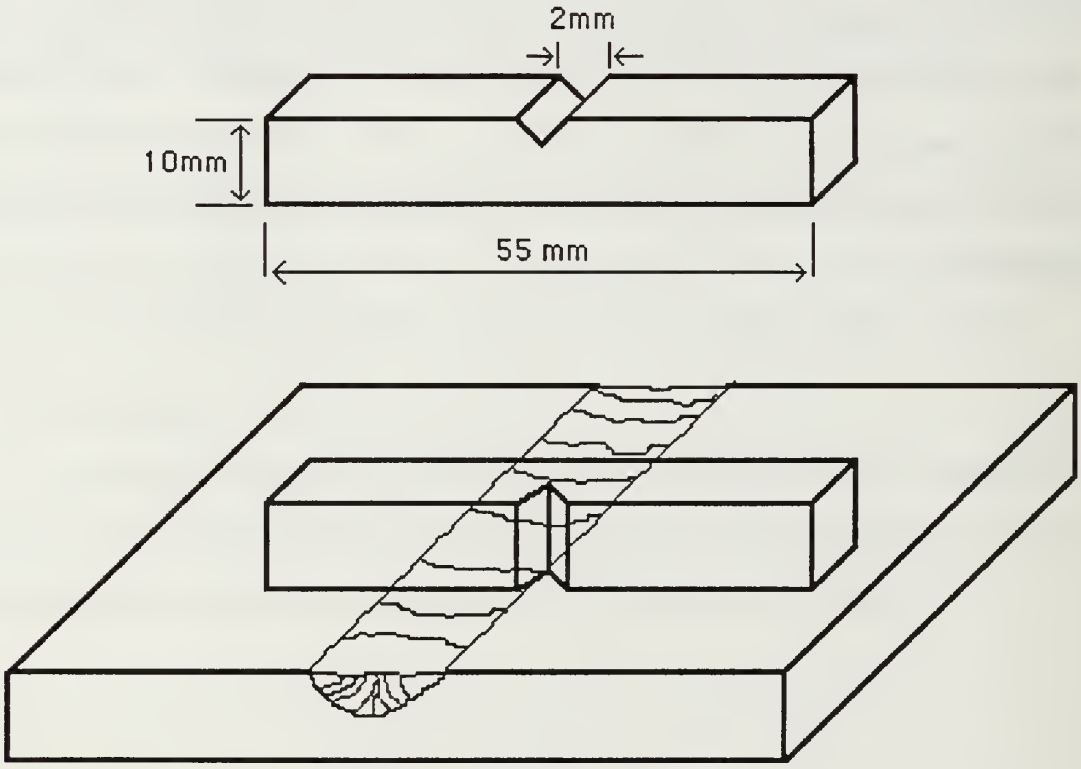

Figure 3.1 Charpy Weldment Sample Orientation

Table 3.1 SAMPLE COMPOSITION DATA

Mat'l ID	C	Mn	Mo	Ni	Nb	Cr	Ti
26A4	0.018	1.44	2.44	2.46	0.06	0.02	0.009
29B4	0.023	1.38	2.26	4.3	0.05	0.22	0.009
32B3	0.028	1.47	2.44	3.45	0.05	0.23	0.007
49A3	0.022	2.02	2.46	5.03	0.05	0.47	0.012
49A4	0.022	2.02	2.46	5.03	0.05	0.47	0.012
49AR	0.022	2.02	2.46	5.03	0.05	0.47	0.012
49B3	0.022	2.02	2.46	5.03	0.05	0.47	0.017
49B4	0.022	2.02	2.46	5.03	0.05	0.47	0.017
49C3	0.022	2.02	2.46	5.03	0.05	0.47	0.024
49C4	0.022	2.02	2.46	5.03	0.05	0.47	0.024
50B3	0.019	1.98	2.26	5.01	0.04	0.47	0.011
50B4	0.019	1.98	2.26	5.01	0.04	0.47	0.011
51A1	0.027	1.98	1.47	6.07	0.04	0.49	0.01
51B3	0.027	2.47	2.91	6.07	0.04	0.49	0.01
51B4	0.027	2.47	2.91	6.07	0.04	0.49	0.01
51C2	0.027	2.44	2.87	6.07	0.04	0.49	0.01
75A3	0.022	1.96	1.57	5.04	0.04	0.49	0.011
75A4	0.022	1.96	1.47	5.04	0.04	0.49	0.011
75B3	0.022	1.87	2.97	5.07	0.04	0.49	0.011
75B4	0.022	1.87	2.97	5.07	0.04	0.49	0.011
75C3	0.022	1.77	4.83	5	0.04	0.49	0.011
75C4	0.022	1.77	4.83	5	0.04	0.49	0.011

All amounts in weight percent.

B. TESTING PROCEDURES

The Naval Surface Warfare Center, Annapolis Detachment conducted initial tests and collected data on the samples. These experiments included Rockwell Hardness (Rc), percent elongation (El'n), reduction in area (RA), Charpy V-Notch Upper Shelf Energy (CVN USE), and Fracture Appearance Transition Temperature (FATT) as shown in APPENDIX B - Measured Data on page 53.

The Rockwell Hardness test measures the resistance to penetration of the surface of a material by a hard object. It is used primarily as a basis for comparison of the different alloy steels, quality control, and correlation with other properties and behavior of materials. However there is a linear relationship between hardness and the Tensile strength of the material.

Ductility is determined by the Percent Elongation and Reduction in Area measurements which is simply a recording of the materials ability to deform.

The Charpy V-Notch Upper Shelf Energy measures the ability of the material to withstand a sudden blow. The degree to which it absorbs the impact energy is a measure of its toughness. At high temperatures a material typically behaves in a ductile manner with a high degree of deformation and stretching prior to failure. At low temperatures, materials typically become brittle, and little deformation takes place before fracture. The transition from ductile to brittle often takes place within a narrow range of temperatures with the median point known as the Fracture Appearance Transition Temperature (FATT).

Specimens were then shipped to the Naval Post Graduate School for further testing and analysis. Each sample was coarsely sanded using a succession of finer sandpapers. They were then finely polished on polishing wheels using 6μm and 1μm diamond paste abrasive. The samples were then etched using a 5% nital solution for an average of 70 seconds to visually define the weld and Heat Affected Zone (HAZ).

The macrostructure of the weld area was observed and photographed using an optical microscope. Both the top and axial sides of the weld area were prepared in order to observe the weld grain growth characteristics. In addition low power large depth of focus optical fractographs of the Charpy surfaces were taken.

The fracture surface of the unpolished half of the Charpy samples were observed under a Cambridge Stereo Scan S200 Scanning Electron Microscope (SEM). The SEM was operated using a Tungsten filament. The accelerating voltage was 20 KV and the specimen working distance was 18mm. Inclusion composition was determined using a Kevex 8000 Energy Dispersive X-ray (EDX) analysis spectrometer in conjunction with the SEM.

Experimental data was manipulated and plotted in various ways to see the effect of the differing compositions upon the mechanical properties observed.

IV. RESULTS AND DISCUSSION

A. MECHANICAL PROPERTIES

The mechanical properties of the ULCB weldments were quite varied over the realm of samples as tabulated in Table 4.1 below and shown graphically in Figure 4.1 and Figure 4.2 The wide scatter of data gives no direct information of the cause of embrittlement.

	Yield Strength		Tensile		CVN USE		FATT	Ductility	
Mat'l ID	KSI	MN/m^2	KSI	MN/m^2	ft-lb	N-m	°F	% El'n	% RA
26A4	106	730.85	123	848.06	180	244.06	20	21	70
29B4	122	841.17	130	896.32	145	196.6	15	17	74
32B3	114	786.01	123	848.06	150	203.38	-10	23	77
49A3	125	861.85	133	917.01	120	162.7	0	18	62
49A4	125	861.85	133	917.01	125	169.48	0	21	53
49AR	115	792.90	134	923.90	82	111.18	40	18	71
49B3	111	765.32	130	896.32	100	135.59	30	19	66
49B4	124	854.96	137	944.59	130	176.26	30	14	63
49C3	120	827.38	138	951.48	120	162.7	20	19	66
49C4	115	792.90	138	951.48	102	138.3	75	16	67
50B3	122	841.17	134	923.90	80	108.47	60	21	74
50B4	127	875.64	157	1,082.48	40.1	54.371	120.1	15	44
51A1	127	875.64	136	937.69	95	128.81	0	21	58
51B3	118	813.59	139	958.38	60	81.352	75	19	70
51B4	123	848.06	157	1,082.48	40.1	54.371	100	17	55
51C2	136	937.69	153	1,054.90	110	149.15	80	14	62
75A3	111	765.32	129	889.43	110	149.15	-10	24	71
75A4	111	765.32	137	944.59	90	122.03	20	21	66
75B3	113	779.11	158	1,089.38	35.1	47.591	120.1	16	55
75B4	135	930.80	148	1,020.43	100	135.59	55	19	59
75C3	128	882.53	147	1,013.54	80	108.47	65	18	64
75C4	128	882.53	147	1,013.54	40.1	54.371	125	18	64

Table 4.1 Thesis Data Summarization

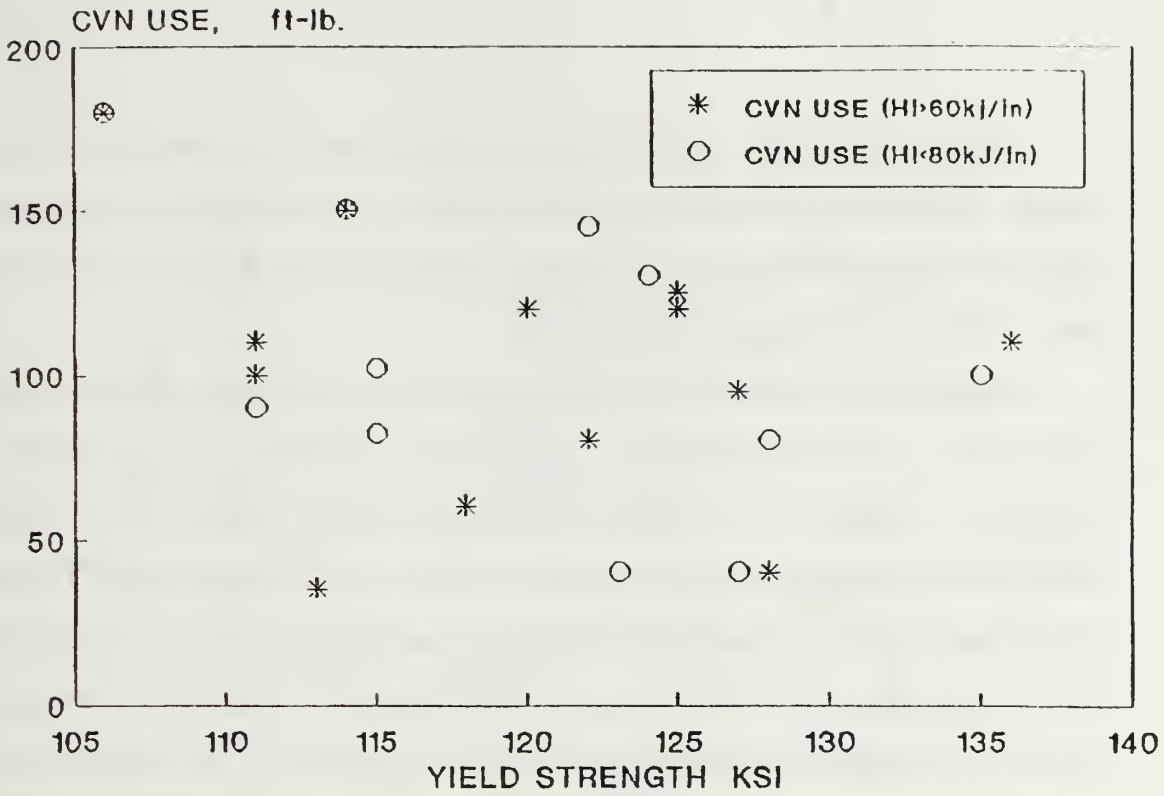

Figure 4.1 CVN USE vs. Yield Strength

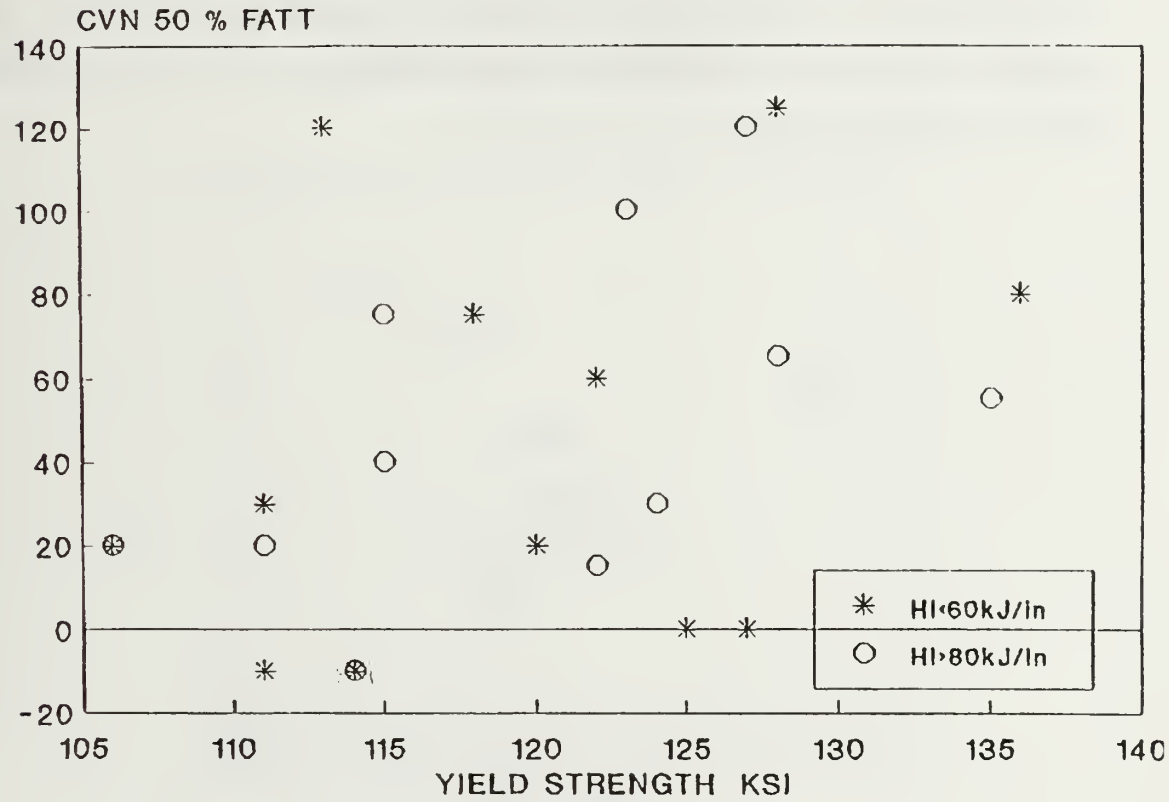

Figure 4.2 CVN 50% FATT vs. Yield Strength

Analysis of the Mn and Ni compositions demonstrated that they increased tensile strengths as expected but had little to no contribution to embrittlement. Figure 4.3 through Figure 4.10 display the minimal effects that Mn and Ni had on the resulting FATT or Upper Shelf Energy.

Molybdenum however showed a consistent contribution to loss in ductility. This effect was more pronounced in the lower 50KJ/in power rate graphs. As displayed in Figure 4.11 we see a decreasing impact energy with increasing Molybdenum weight percent. Likewise in Figure 4.12 we see the FATT increase nearly linearly with an increase in Molybdenum alloying content. The reason for this effect is not yet understood. One possible mechanism is that an increase in the molybdenum causes a greater degree of Mo migration to the solidifying weld columnar boundaries as discussed below. A harder, more brittle molydenum containing phase could form at these columnar grain boundaries and act to propagate a crack rather than block its path. An example of this type of columnar failure is illustrated in Figure 4.19 on page 35.

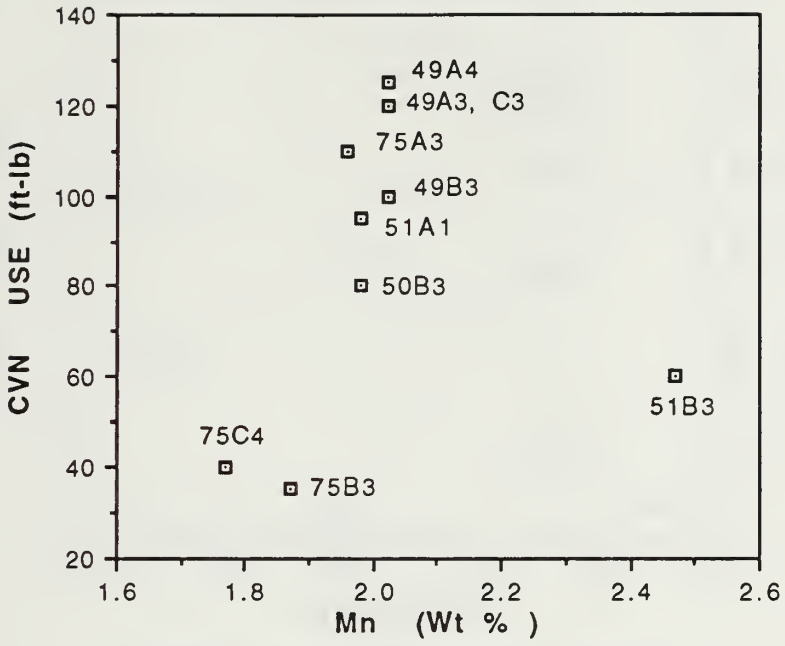

Figure 4.3 USE vs. Mn content

50KJ/in heat input

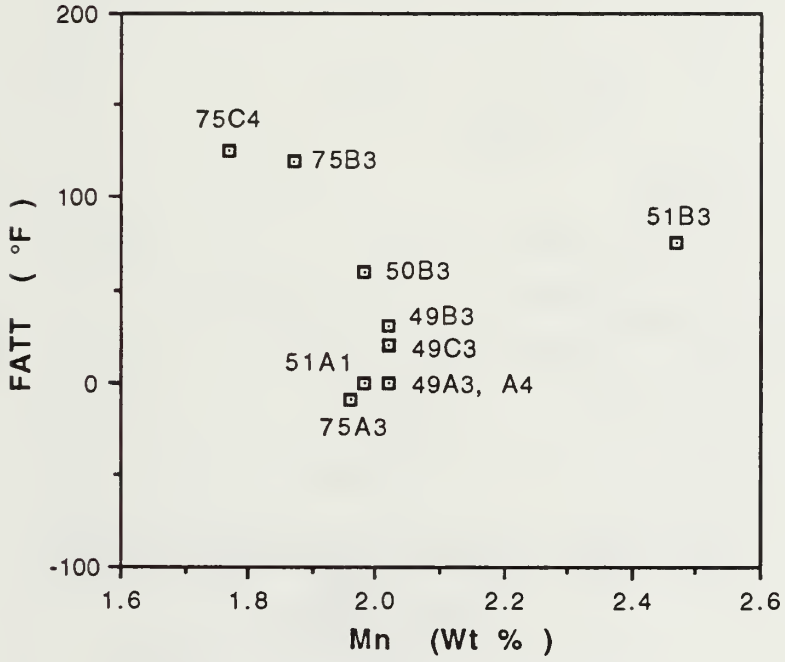

Figure 4.4 FATT vs. Mn content

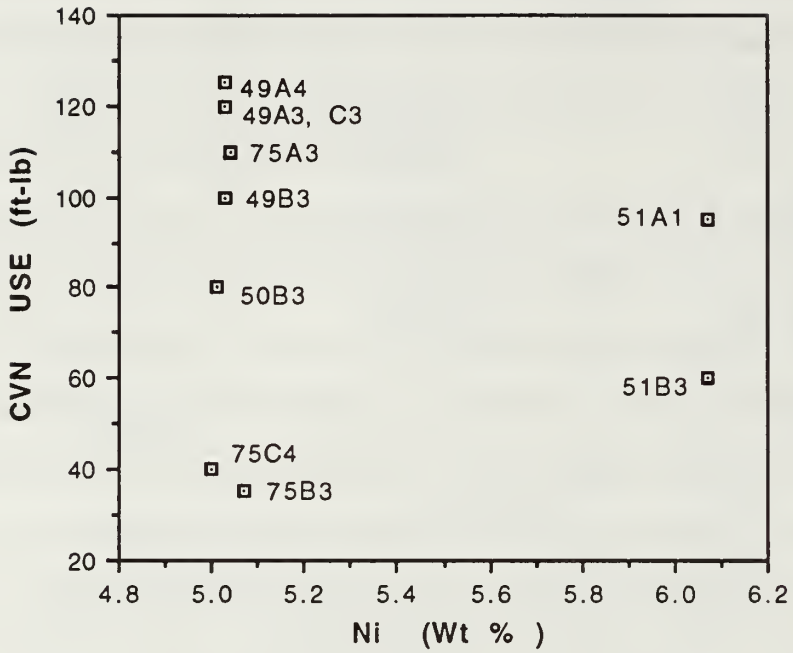

Figure 4.5 USE vs. Ni content

50KJ/in heat input

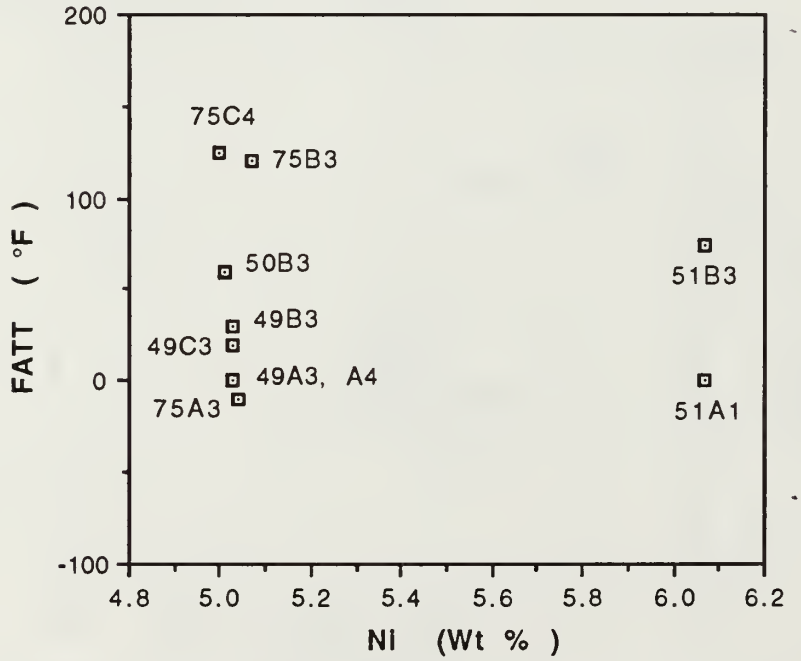

Figure 4.6 FATT vs. Ni content

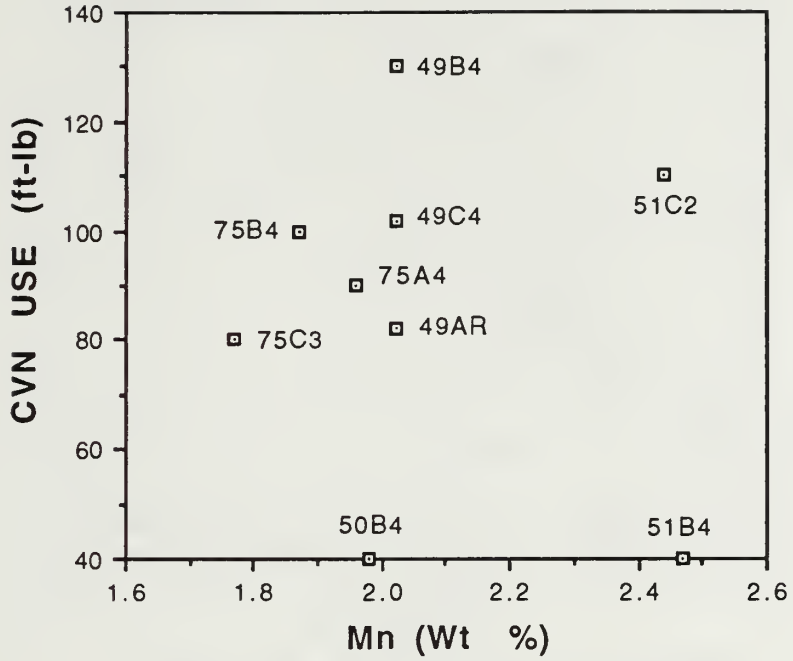

Figure 4.7 USE vs. Mn content

100KJ/in heat input

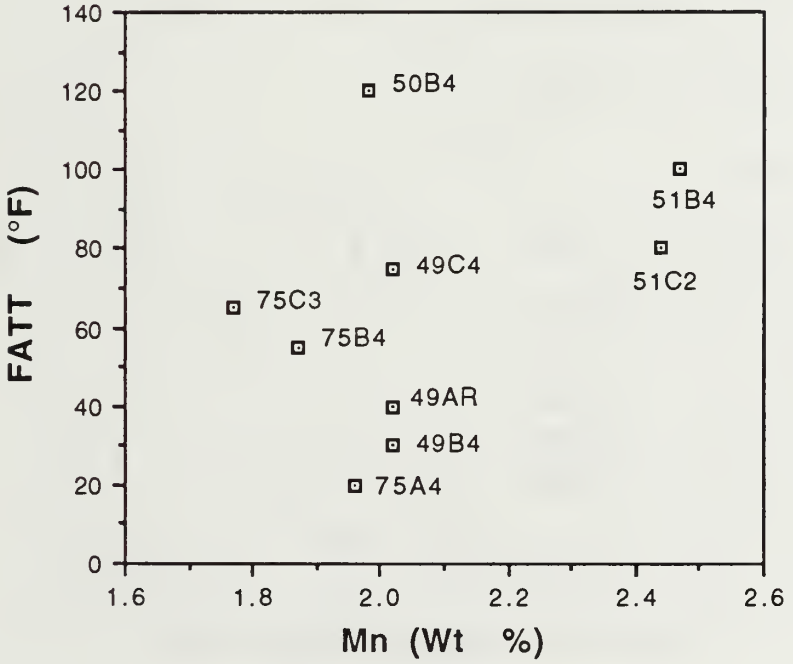

Figure 4.8 FATT vs. Mn content

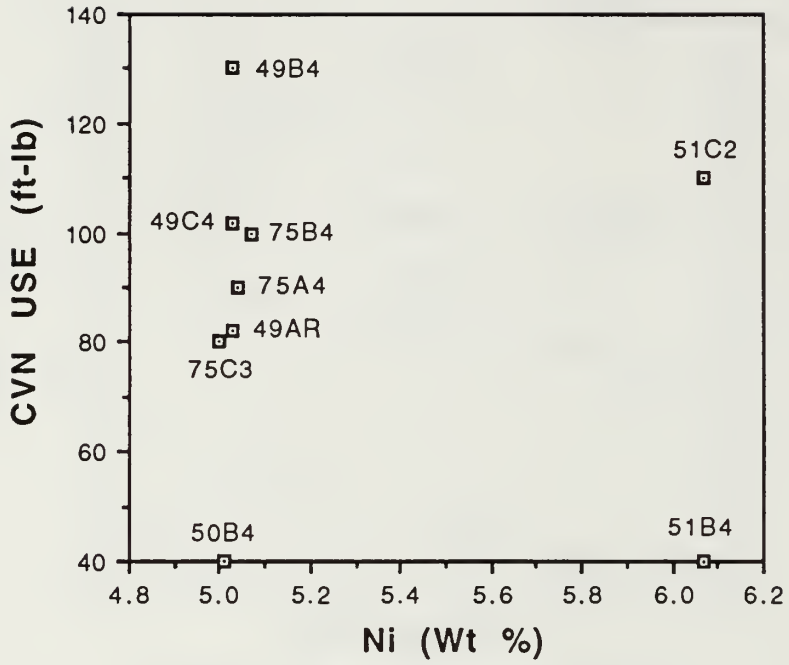

Figure 4.9 USE vs. Ni content

100KJ/in heat input

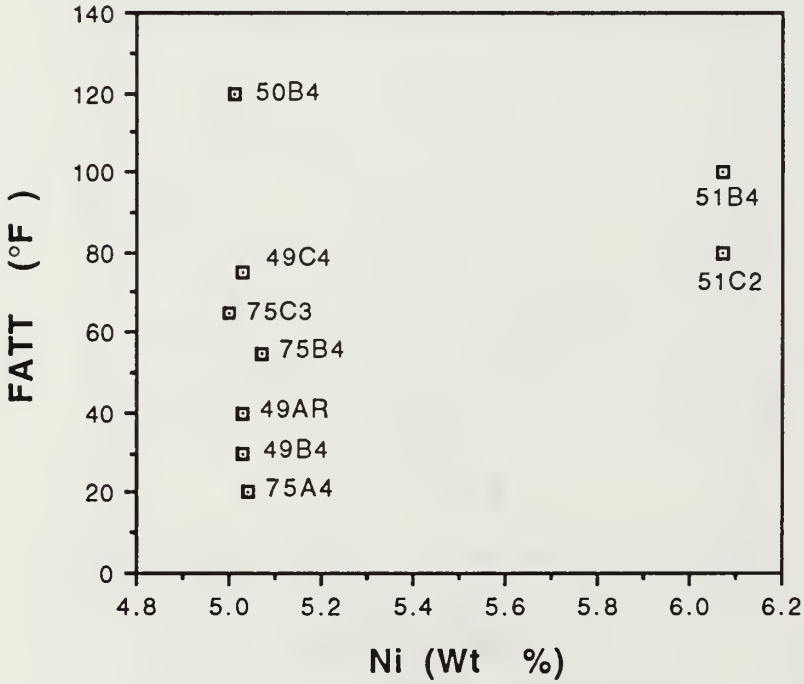

Figure 4.10 FATT vs. Ni content

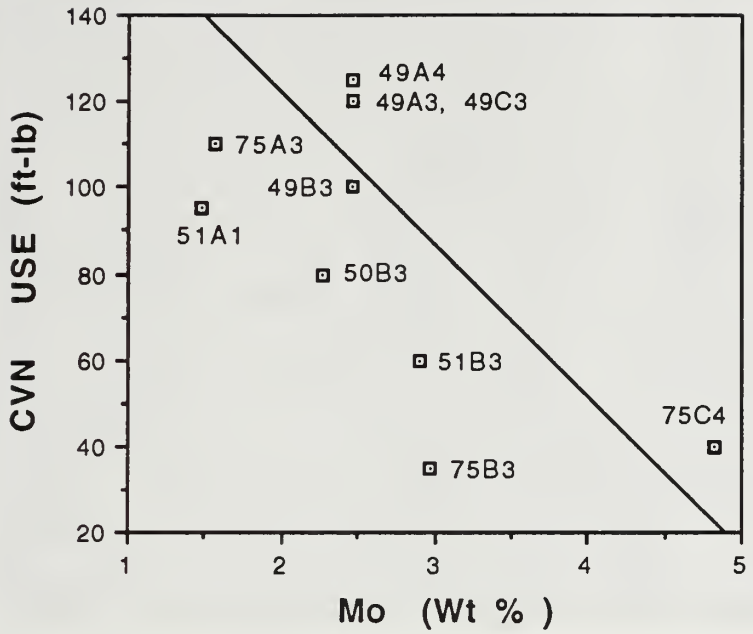

Figure 4.11 CVN USE vs. Mo content

50KJ/in heat input

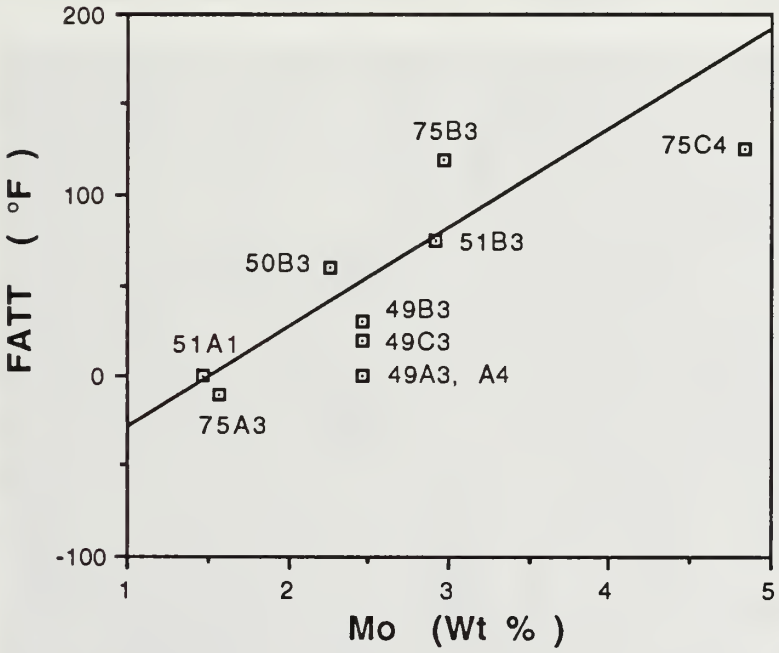

Figure 4.12 FATT vs. Mo content

B. MACROSTRUCTURAL ANALYSIS

The grain structure of the solidified weld and heat affected zone demonstrated an increasing columnar grain growth associated with those samples having a more brittle behavior. In Figure 4.13 and Figure 4.14 we see distinct columnar growth associated with a lower heat input. Weld pool solidification initially begins at the fusion boundary as the partially melted base metal grains serve as nucleation sites for columnar growth. The grain grows in the weld pool in the direction of maximum temperature gradient and normal to the fusion line. A more rapid cooling rate is created due to the lower heat input and thus a larger temperature gradient ensues. A lower degree of constitutional supercooling accompanies this larger temperature gradient and results in larger columnar and dendritic growth structures.

Constitutional supercooling in alloy solidification and the interaction of the temperature gradient with the degree of constitutional supercooling is illustrated in Figure 4.15. Characteristic dendritic growth proceeds until the subcooled liquid next to the solidification front reaches equilibrium temperature.

A higher heat input rate provides a slower cooling rate and a lower temperature gradient in the weld pool. A larger region of constitutional supercooling is created due to the reduced temperature gradient and fully equiaxed grains are then permitted to form. The formation of solid nuclei in front of the solid-liquid interface is increasingly encouraged by the expanding constitutional supercooling region due to an increasing heat input. The differing solidification structures of weld metal as the supercooling is increased is illustrated in Figure 4.16. In addition successive passes in higher power welds serve to refine previous columnar grains by reaustenitizing and thus recrystallizing them so that they are small and equiaxed.

Figure 4.13 Optical macrograph of flat-etched sample 75B3-9
Top of the weld in upper picture, side of weld in lower picture,(8x mag.)

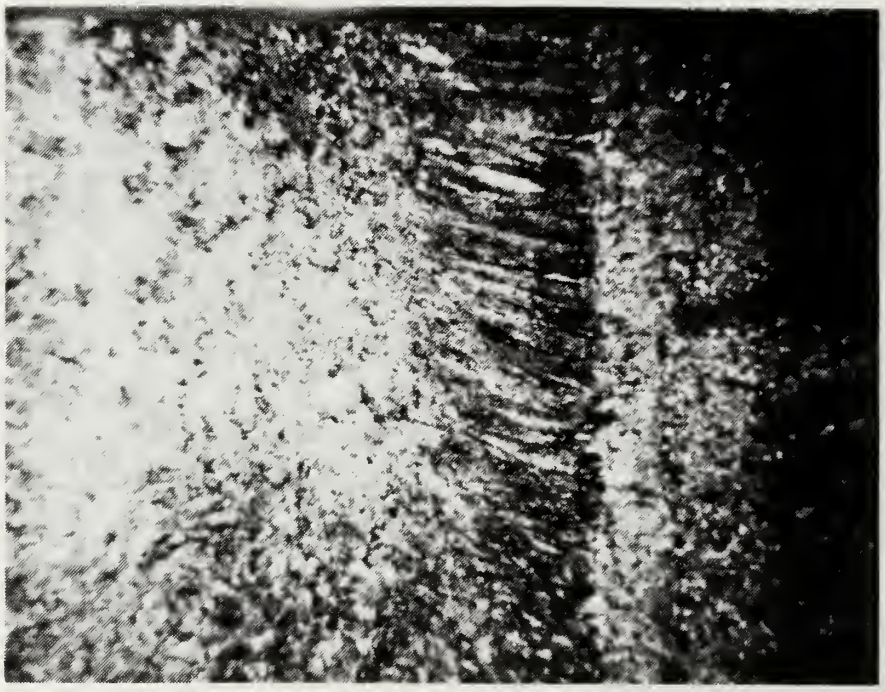

Figure 4.14 Optical macrograph of flat-etched sample 75B3-8
(5% nital etch, 8x mag.)

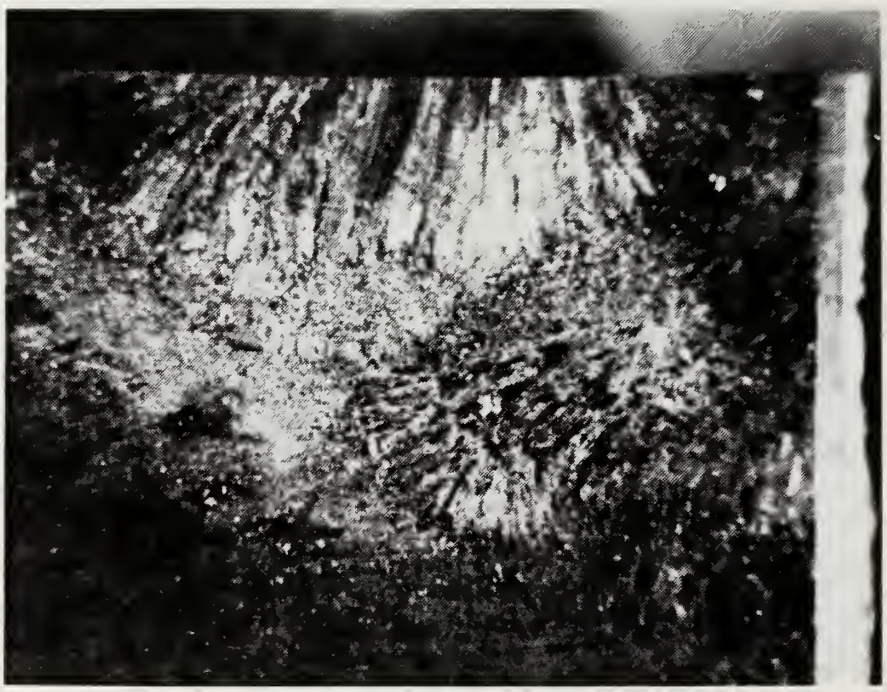

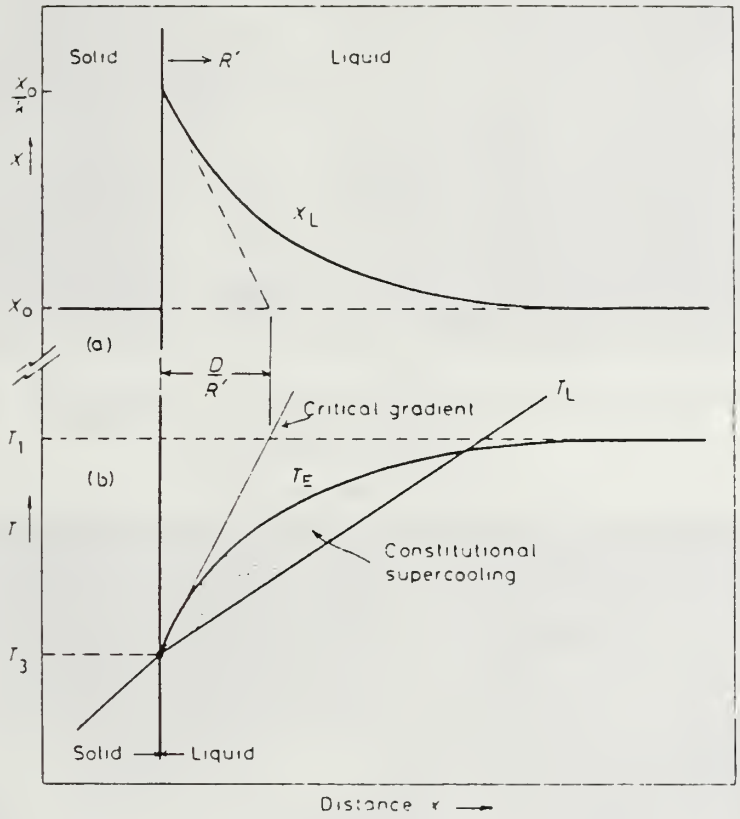

Figure 4.15 Constitutional supercooling in alloy solidification
Easterling, 1983, p.66

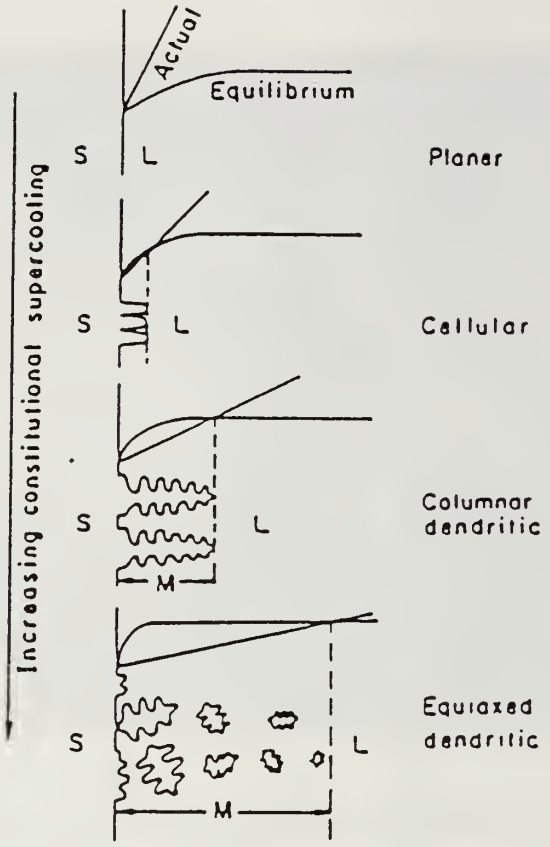

Figure 4.16 Solidification structure of weld metal with increasing supercooling
(Kou, 1987, p.135)

Figure 4.17 and Figure 4.17 illustrate the higher proportion of equiaxed grains and fewer columnar grain structures associated with higher heat input weldings. In this case successive passes appear to have recrystallized and/or remelted the previously laid down weld metal so that there are large amounts of tough equiaxed grains. Here columnar microstructures only dominate in the final weld pass. Test results for this ULCB steel also showed a relatively higher ductility and toughness.

Figure 4.17 Optical macrograph of flat-etched sample 75A4-5
(5% nital etch, 8x mag.)

Figure 4.18 Optical macrograph of flat-etched sample 75A4-11
(5% nital, 8x mag.)

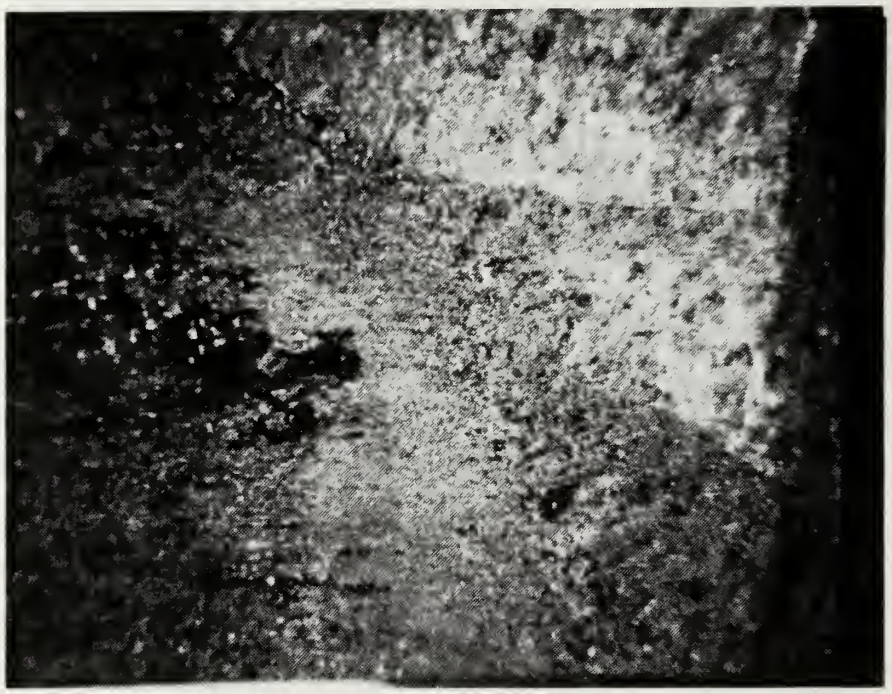

Figure 4.19 shows the fracture surface of one of the more brittle specimens. Here the inter-columnar crack failure mode is quite visible. Note the towering protrusions and shear cliffs as indicated by the dark shadows they produce. A deep valley region can be seen in the upper left.

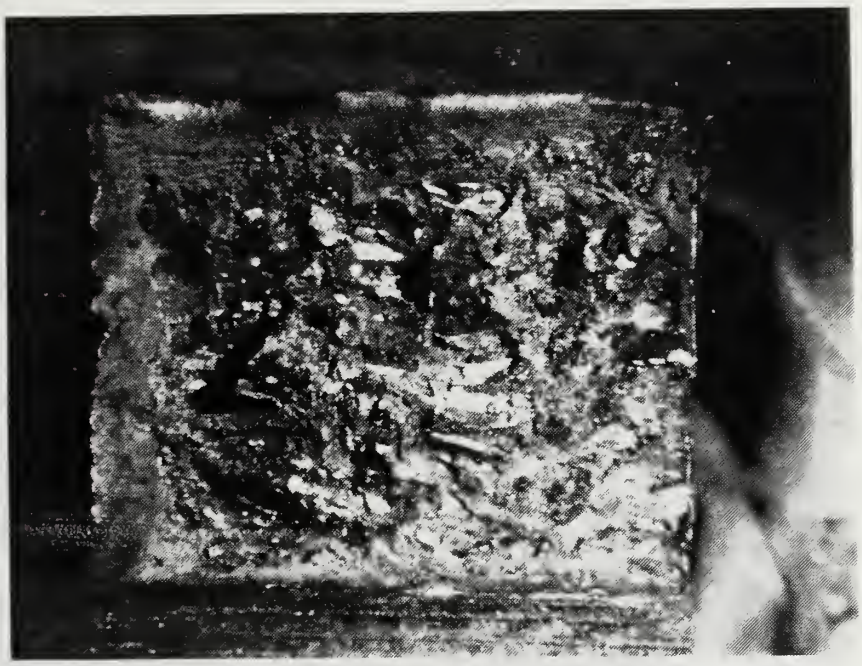

Figure 4.19 Very Brittle fractograph sample 50B4-10

(7.5x mag.)

C. MICROSTRUCTURAL ANALYSIS

1. Inclusions

A cross section of the ULCB weldment samples were evaluated using an optical, scanning electron microscope (SEM). Figure 4.20 illustrates a classic ductile fracture with the deposit of inclusions indicating the sites of initial microvoid formation. Several different types of inclusions were identified based on their chemical composition and contained the following elements in the form of oxides.

Al,Cr, Mn, Mo S, Si, and Ti

Typical inclusions were found to average around 1 micron in diameter and be of complex manganese-alumino-silicate and alumino-silicate compositions. A typical EDX analysis of these inclusions is shown in Figure 4.21 and Figure 4.22.

The more brittle specimens are typified by sample 50B4-10 shown here in a series of SEM fractographs in Figure 4.23 through Figure 4.25. These brittle samples showed a combination of cleavage and inter-columnar crack propagation. This specimen is the same as that shown in Figure 4.19 on page 35. The large cliffs and valleys indicative of columnar cracking is evident. In all samples at least a small amount of dimpled, ductile fracture region was visible at higher temperatures as seen here the higher magnification SEM fractographs Figure 4.24 and Figure 4.25.

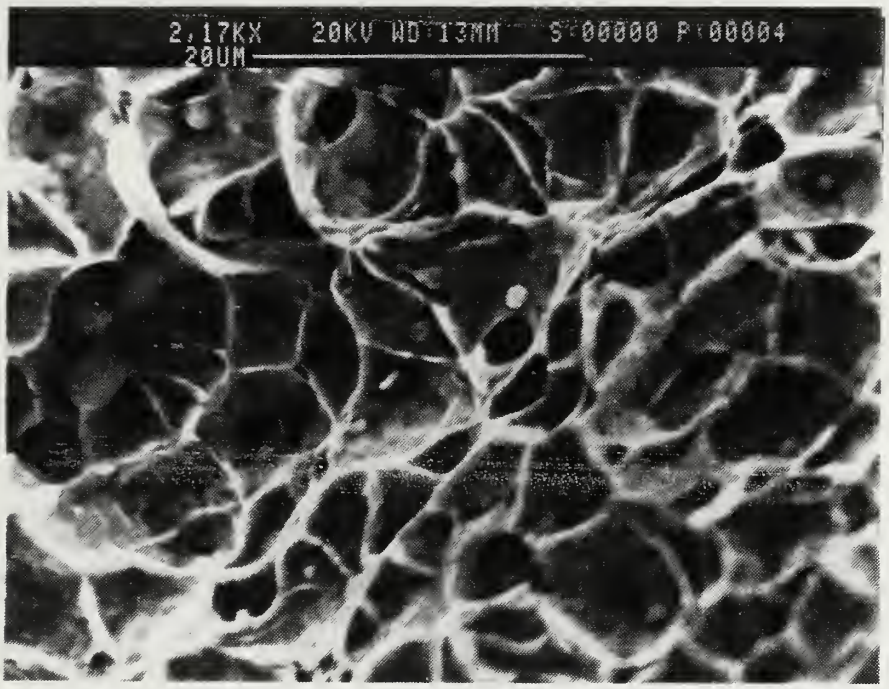

Figure 4.20 Ductile fracture specimen 49B3-1

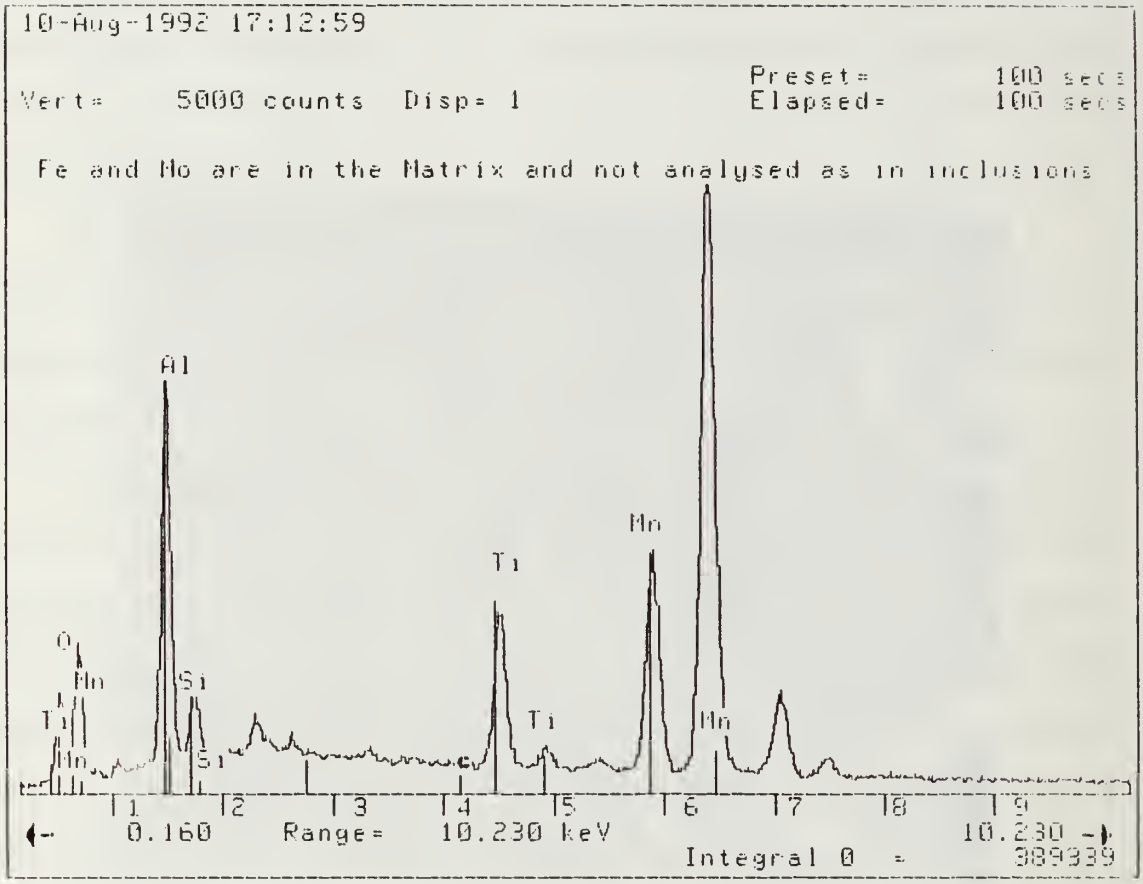

Figure 4.21 EDX Graph of 49B3-1.

Typical of compositions of inclusions in all samples

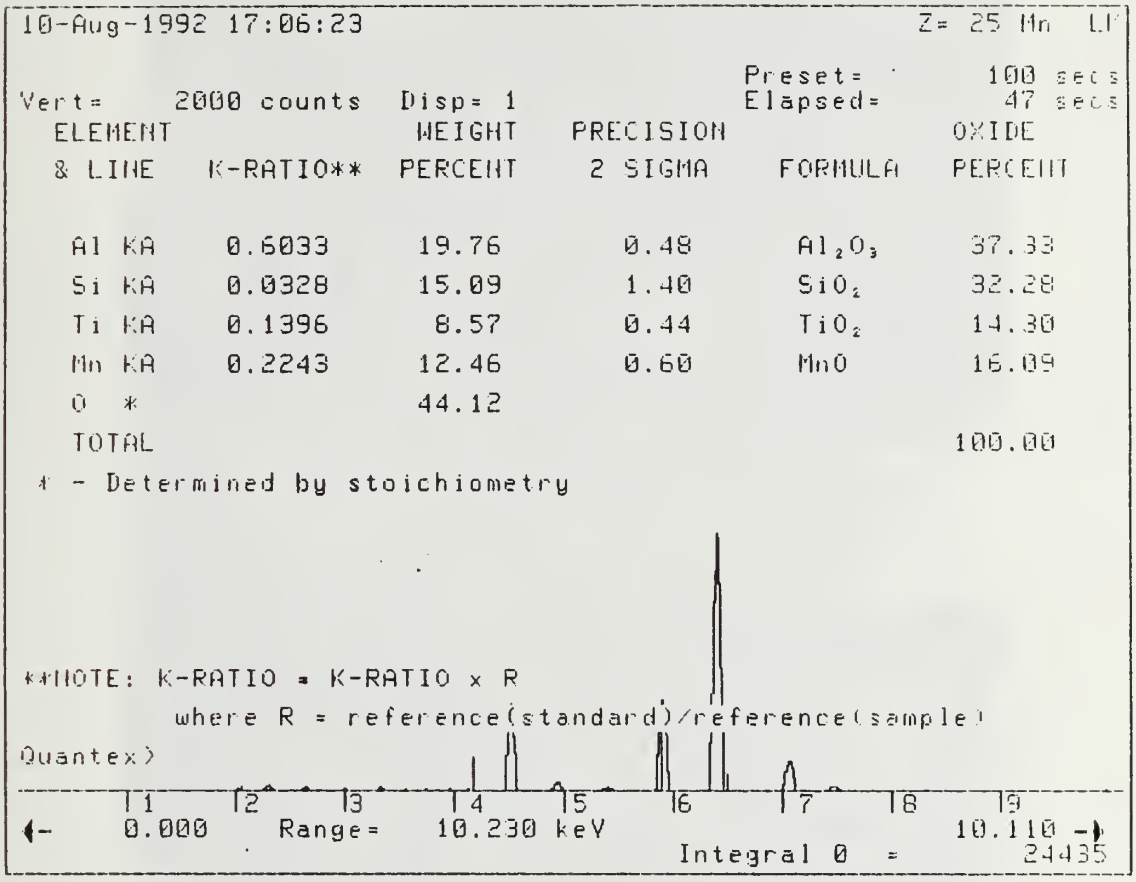

Figure 4.22 EDX Data of 49B3-1

Typical of compositions of inclusions in all samples

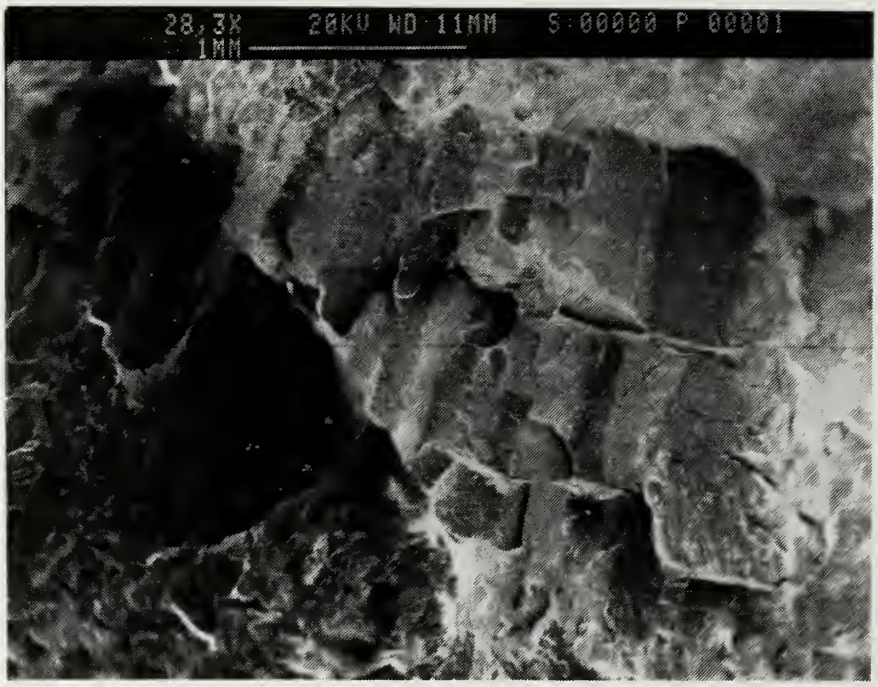

Figure 4.23 SEM micrograph of 50B4-10

An example of Quasi-Cleavage in an embrittled sample

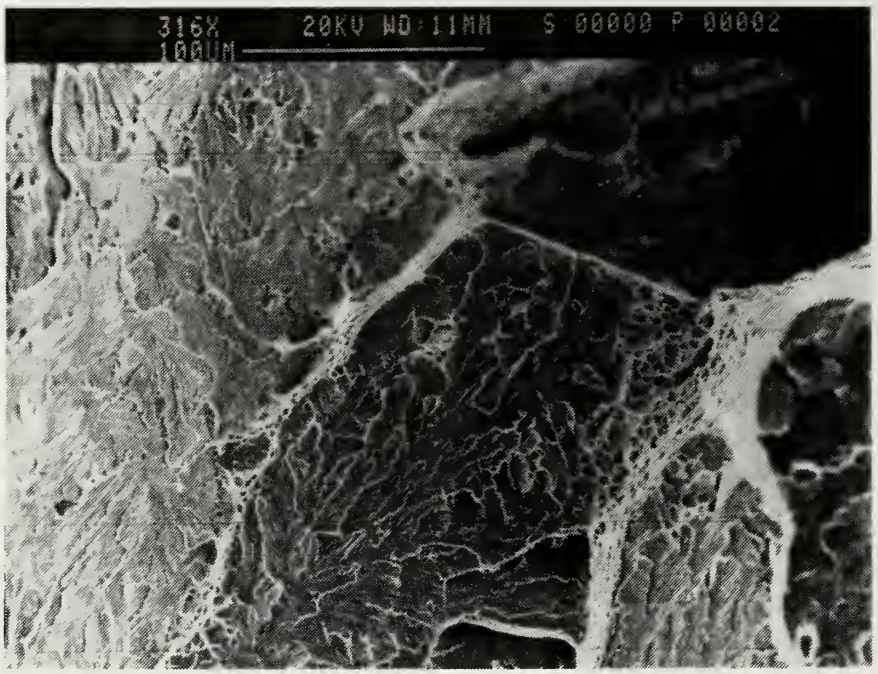

Figure 4.24 SEM of 50B4-10 at medium magnification

This is a closer shot of the center of Figure 4.23 above.

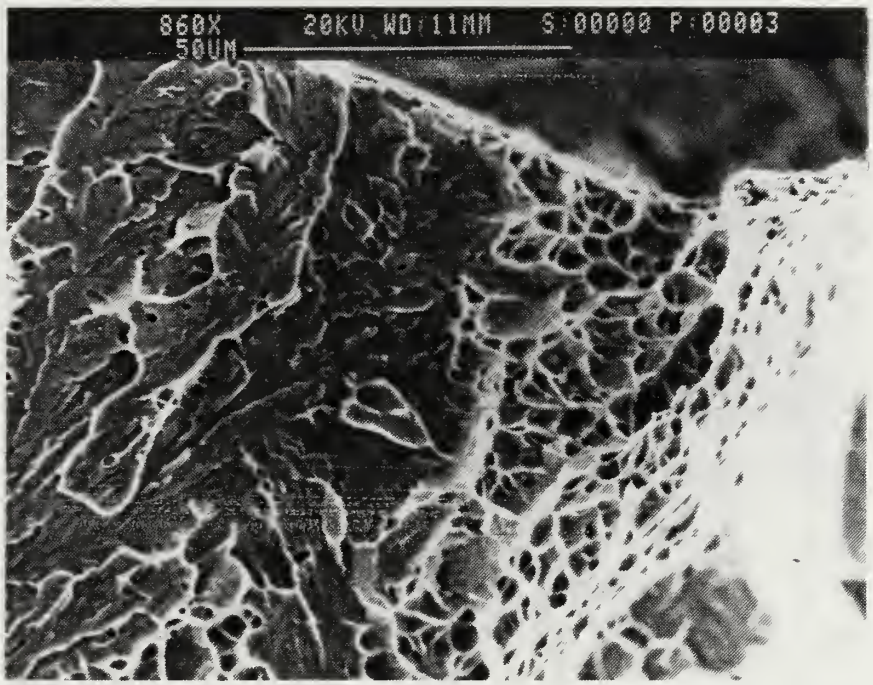

Figure 4.25 SEM of 50B4-10 at high magnification

A small amount of ductile fracture is still visible even on the brittle samples

D. DATA ANALYSIS AND MATHEMATICAL MODELING

Many of the following calculations were performed with the exclusion of the erroneous readings obtained from the extremely brittle samples. Samples with FATT's in excess of 100°F were considered embrittled and disregarded unless otherwise specified below. Proceeding in this way a much more consistent pattern in the measured properties was observed.

1. Tensile Strength vs. FATT

As shown in Figure 4.26 there was a largely consistent trend for the Fracture Appearance Transition Temperature (FATT) to increase with rising Tensile Strength in the material.

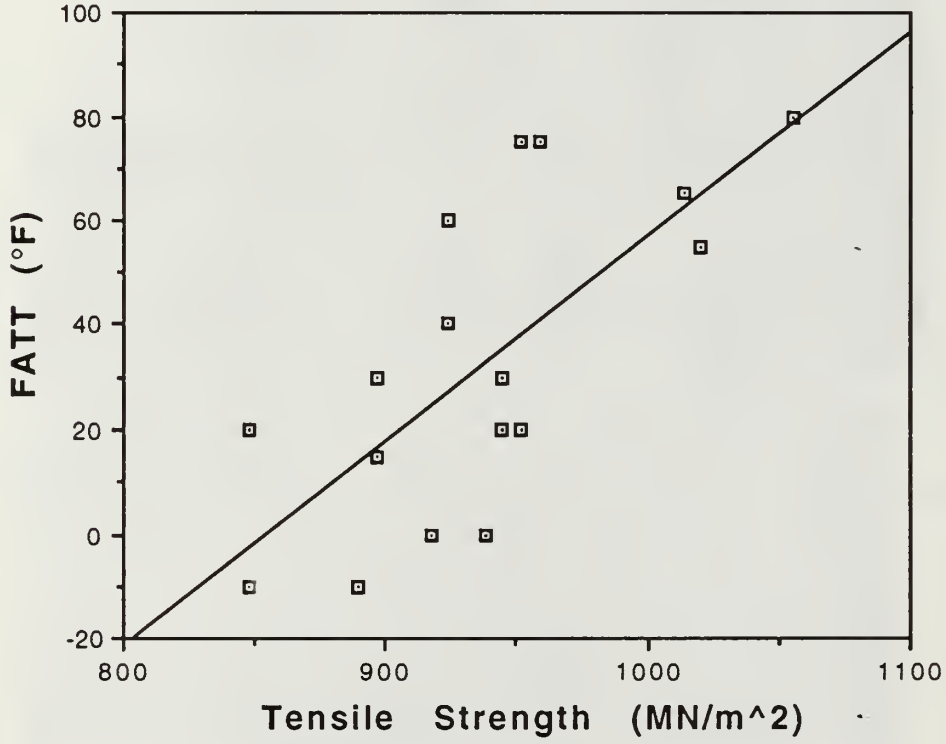

Figure 4.26 FATT vs. Tensile Strength for all data.

2. Yield Strength to Tensile Strength Ratio

Figure 4.27 below shows the resulting Yield strength to tensile strength ratio. Without the embrittled data the strengths are consistent averaging a Y/S ratio of 0.887.

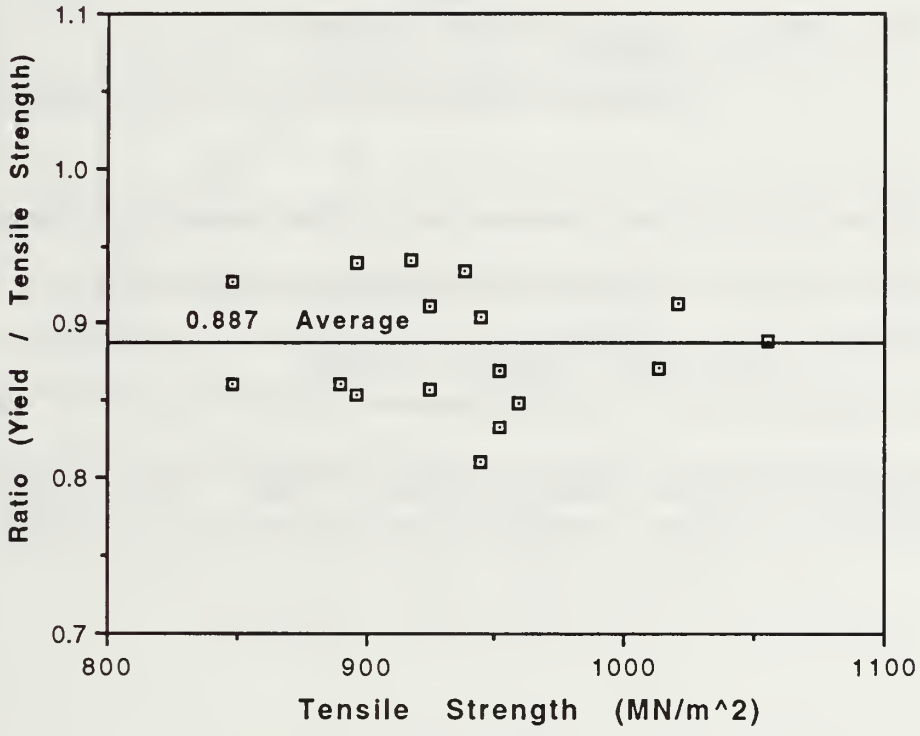

Figure 4.27 Yield to Tensile Strength Ratio

3. Modified Pickering Tensile strength calculation as a function of Alloy Content.

Professor Brian Pickering having conducted experiments on low carbon steels within the range of 0.05 - 0.2 wt% carbon empirically derived the following formula to predict the tensile strength obtained from the materials composition (Pickering, 1978, p.106).

$$\text{T.S. } (MN/m^2) = 15.4[16 + 125(C) + 15(Mn + Cr) + 12(Mo) + 6(W) + 8(Ni) + 4(Cu) + 25(V + Ti)]$$

The ULCB steels in this study however had carbon contents in the range 0.018 - 0.022 wt%. In order to fit the low carbon data a correction factor of 0.52 was calculated and applied to the Pickering formula. As can be seen in Figure 4.28 this Modified Pickering formula is in good agreement in predicting ULCB steel Tensile Strength. A small amount of scatter is expected considering the steel is in the form of a weldment, a much less controlled process than steel plate production.

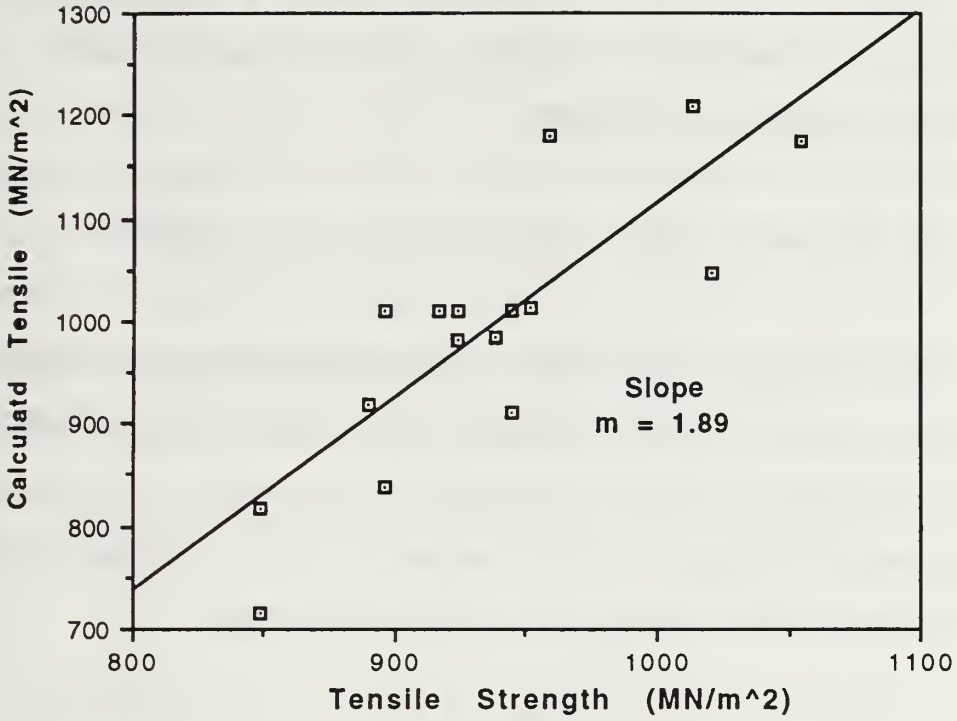

Figure 4.28 Mod. Pickering Tensile Strength Calculation.

$$\text{T.S. (MN/m}^2) = 15.4\ (0.52)[16 + 125(C) + 15(Mn + Cr) + 12(Mo) + 6(W) + 8(Ni) + 4(Cu) + 25(V + Ti)]$$

4. Tensile Strength vs. Bainitic Start Temperature.

Professor Pickering also empirically derived a formula to predict the Bainite start temperature of an alloying mix as a function of the alloying percentages. (Pickering, 1978, p.105)

$$B_S\ °C = 830 - 270(C) - 90(Mn) - 37(Ni) - 70(Cr) - 83(Mo)$$

It was recognized that as the transformation temperature was lowered the strength increased in a linear relationship. Thus a higher strength weldable steel could be obtained if the bainite start temperatures were reduced. As shown in Figure 4.29 the trend of Pickering's formula, if not the accuracy, is supported by the present data even though derived from steels of 0.05 to 0.2 carbon.

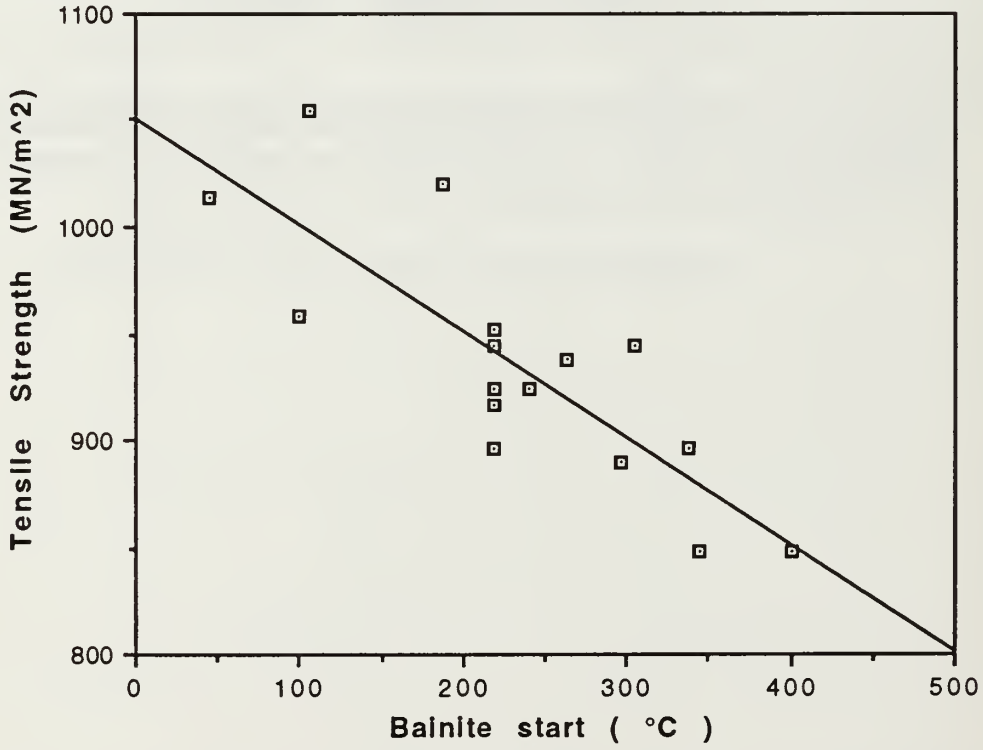

Figure 4.29 Tensile vs. Bainitic Start Temp.(w.o embrittled data)

5. Calculated Mo effect of Tensile Strength using the Mod. Pickering Formula.

Using the Mod Pickering formula the effect of the change in Mo on the Tensile strength was then sought. The strength increment due to the Mo was extracted and plotted vs. FATT & USE for 50KJ/in, 100KJ/in and all powers. This is shown in Figure 4.30 through Figure 4.32. These show that Mo is clearly responsible for embrittlement and that this is much worse for low power weldments. It would seem that the increasing number of equiaxed recrystallized grains has offset the embrittling effects of Mo in the high power weldments

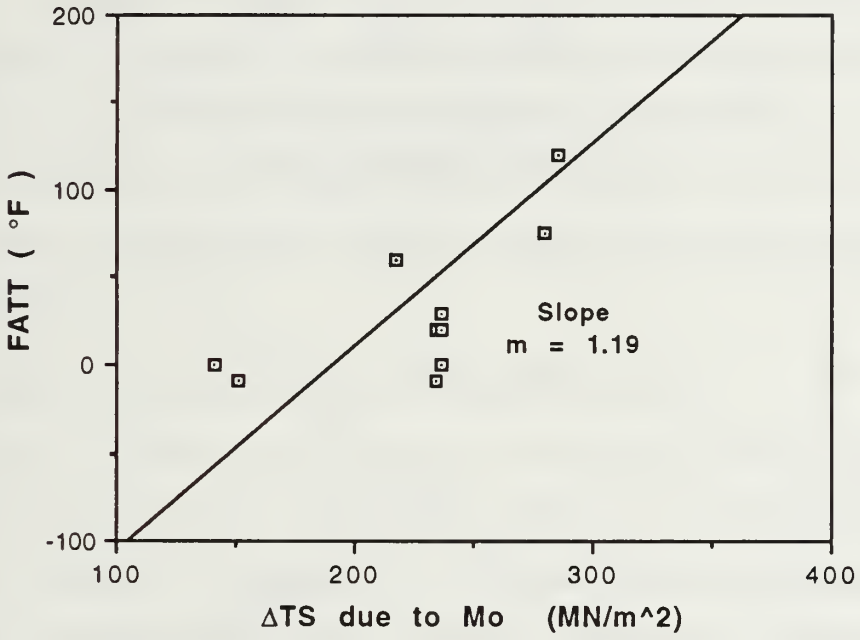

Figure 4.30 Change in Tensile Strength due to Mo content vs. FATT

(50 KJ/in heat input)

$TS(MN/m^2) = 15.4(0.52)[12(Mo)]$

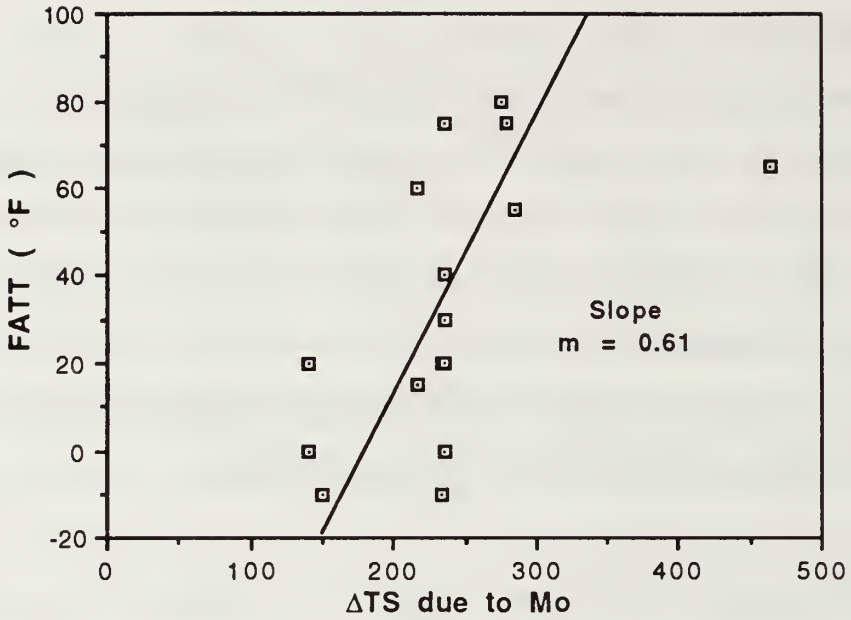

Figure 4.31 ΔTS due to Mo vs. FATT

(50 & 100 KJ/in heat input)

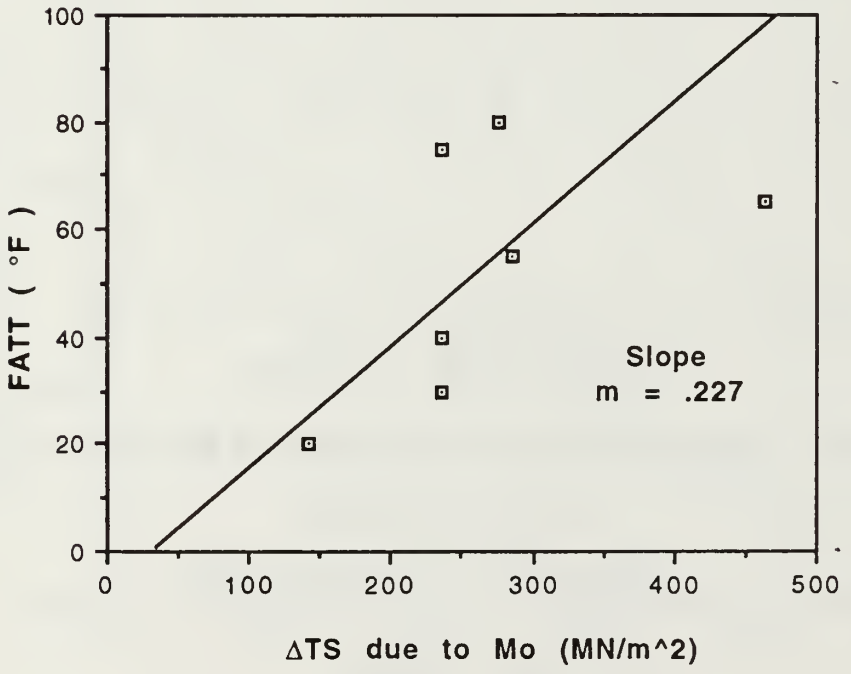

Figure 4.32 ΔTS due to Mo vs. FATT

(100KJ/in heat input)

V. SUMMARY

A. CONCLUSIONS

1. Weld Metal Compositions

The ULCB steels are successful in achieving the required strengths when used as weld metal provided appropriate metal compositions are chosen. The alloying elements in ULCB weld wire can lead to weld metal embrittlement in particular the addition of molybdenum.

2. Weld Metal Heat Input

Increasing the power in multi-run TIG weldments on ULCB steels seems to improve the toughness by reducing the amount of columnar grains in the weld metal. Through the use of successive passes the weld metal attains a greater degree of recrystallization and the higher proportion of equiaxed grains aids in increasing the fracture toughness of the material and this also can offset the effects of Mo embrittlement.

B. RECOMMENDATIONS FOR FUTURE STUDY

Since it is evident that high powers and increased amounts of recrystallized equiaxed grains improve toughness the influence of electrode powers upon the relative proportion of columnar and recrystallized microstructures should be studied. A detailed analysis of the fractions of columnar to equiaxed grain areas produced by differing heat input rates should be conducted and implications on toughness explored.

Development of an alloy with a lower upper critical transformation temperature would increase the likelihood of recrystallization in the weld and at the same time would depress the Bainite Start Temperature. This could be attained most likely with higher proportions of nickel and manganese in the alloy composition.

To avoid embrittlement caused by excessive levels of molybdenum ULCB compositions should limited to 2 wt% Mo and be further refined in order to produce a weld metal with optimum strength and toughness over a larger range of weld powers as possible.

APPENDIX A - Scanning Electron Microscopy

The Scanning Electron Microscope (SEM) was used after optical microscopy to take fractographs of the fracture surfaces of the different samples. Secondly it was used in conjunction with the KEVEX analyzer to determine the chemical composition of sample inclusions. Several detection processes are available on the SEM providing differing and unique methods of presentation.

The secondary electron (SE) setting is used primarily to give a topographical presentation by collecting low energy secondary electrons. As fast incident electrons collide with sample atoms they eject lightly bounded valence electrons also known as secondary electrons. Due to the low energy levels of these secondary electrons only those located near the surface are permitted to escape the material. Bright images are created by protruding surfaces while canyons retain a higher proportion of secondary electrons and thus appear dark. High atomic number materials have a lower restraint upon secondary electrons and thus appear relatively brighter. Materials with low resistivities retain a beam induced charge and also appear brighter.

The backscattered electron (BSE) setting is used frequently to identify nonmetallic inclusions. The backscattered electrons are created when incident electrons bounce off the nucleus of relatively large atoms. These electrons have a higher energy than the SE electrons and thus are able to escape the sample from areas deep within the sample.

Backscattered electron (BSE) mode was used exclusively for the identification of nonmetallic inclusions. Backscattered electrons are produced from elastic or nearly elastic collisions of incident electrons with the nucleus of a target atom. The BSEs are much more energetic than the secondary electrons and therefore escape

from deeper within the sample. These high energy electrons are used for atomic number or orientation information. The higher the atomic number of an atom, the greater the positive charge of its nucleus. Production of a BSE is more likely to occur and be of higher energy for a large positively charged nucleus. Low atomic number elements show up dark since fewer electrons are backscattered and those that are backscattered have lower energies. Thus, the backscattered electrons may identify the phases present in an inclusion by variations in contrast.

The KEVEX energy dispersive x-ray analyzer was used in conjunction with the SEM. Electrons located in low energy shells of the sample are ejected through collision with generated incident electrons. Another electron within that atom quickly takes the place of the missing electron emitting x-rays as it jumps to a different energy state. Each atom has a distinct pattern in releasing this electromagnetic radiation. These x-rays are then collected by a detector within the SEM vacuum chamber and matched by the KEVEX with the fingerprints of known elements. Through a collection of successive collisions we can also ascertain the relative amount of each element within the sample.

Mat'l ID	Heat Input	Strength Yield	Strength Tensile	Hardness Rc	El'n	RA	CVN USE	FATT	CVN at +30F	Electrode
	kJ/in	ksi	ksi		%	%	ft-lb	F	ft-lb	
26A4	80	106	123	...	21	70	180	20	170	sq. rod
29B4	120	122	130	...	17	74	145	15	145	sq. rod
32B3	80	114	123	25.5	23	77	150	-10	138	sq. rod
49A3	60	125	133	32.0	18	62	120	0	80	sq. rod
49A4	60	125	133	32.0	21	53	125	0		sq. rod
49AR	100	115	134	26.9	18	71	82	40	48	sq. rod
49B3	60	111	130	30.6	19	66	100	30	77	sq. rod
49B4	100	124	137	29.1	14	63	130	30	73	sq. rod
49C3	60	120	138	28.0	19	66	120	20	86	sq. rod
49C4	100	115	138	31.0	16	67	102	75	47	sq. rod
50B3	50	122	134	30.7	21	74	80	60	29	1/16 wire
50B4	100	127	157	33.3	19	44	40.1	120.1	20	1/16 wire
51A1	50	127	136	29.5	21	58	95	0	92	sq. rod
51B3	60	118	139	29.2	19	70	60	75	30	1/16 wire
51B4	100	123	157	33.1	17	55	40.1	100	27	1/16 wire
51C2	100	136	153	34.3	14	62	110	80	30	sq. rod
75A3	50	111	129	27.4	24	71	110	-10	87	1/16 wire
75A4	100	111	137	27.8	21	66	90	20	75	1/16 wire
75B3	50	113	158	28.3	16	55	35.1	120.1	15	1/16 wire
75B4	100	135	148	32.2	19	59	100	55	13	1/16 wire
75C3	100	128	147	34.0	18	64	80	65	30	1/16 wire
75C4	50	128	147	35.7	18	64	40.1	125	23	1/16 wire

LIST OF REFERENCES

Abson, D.J., Dolby, R.E. and Hart, P.H.M., "The Role Of Non-metallic Inclusions I Ferrite Nucleation In Carbon Steel Weld Metals," International Conference on Tren in Steel and Consumables for Welding, The Welding Institute, London, 13-16 November 1987.

Abson, D.J., Pargeter, R.J., "Factors Influencing As-deposited Strength, Microstructu And Toughness Of Manual Metal Arc Welds Suitable For C-mn Steel Fabrications, *International Metals Review*, v.31, No. 4, 1986.

Askeland, D.R., *The Science and Engineering of Materials*, second ed., PWS-KEN 1989.

Blicharski, M.R., Garcia, C.I., Pytel, S. and DeArdo, A.J., "Structure and Properties ULCB Plate Steels for Heavy Section Applications," *Processing, Microstructure ar Properties of HSLA Steels*, The Minerals, Metals, and Materials Society, 1988.

David Taylor Naval Ship Research and Development Center Report, *Pre-Certificati Development Plan HSLA 130 Steel For Submarine Construction*, by J.P. Gudas, Mar 1989.

David Taylor Naval Ship Research and Development Center Report SME-CR-0108 *The Metallurgy of HSLA Steel Weld Metal Produced by the Submerged Arc Process*, D.K. Matlock and G.R. Edwards, March 1985.

David Taylor Naval Ship Research and Development Center Report SME-CR-07-8 *Development of 100KSI Yield Strength HSLA Steel*, by A.P. Coldren and T.B. Cox, Ju 1986.

David Taylor Naval Ship Research and Development Center Report SME-88/62, *Physical Properties, Elastic Constants and Metallurgy of HSLA-100 Steel Plate*, by E Czyryca and Richard E. Link, December 1988.

David Taylor Naval Ship Research and Development Center Report SME-CR-06-8 *Influence of Weld Metal Inclusion Type, Content, and Size Distribution on the Microstructure and Properties of High Strength Steel Weld Metal*, by C.W. Ramsey D.K. Matlock and D.L. Olsen, October 1988.

Edmonds, D.V. and Cochrane, R.C., "Structure-Property Relationships in Bainitic Steels," *Metallurgical Transactions* A, v.21A, June 1990.

Easterling, K., *Introduction to the Physical Metallurgy of Welding*, Butterworths & Co., (Publishers) Ltd., 1983

Grong, O. and Matlock, D.K., "Microstructural Development In Mild And Low-alloy Steel Weld Metals," *International Metals Reviews*, v.31, no.1, 1986.

Grong O., Siewart, T.A., martins, G.P. and Olson, D.L., "A Model for the Silicon-manganese Deoxidation of Steel Weld Metals," *Metallurgical Transactions* A, v.17A, October 1986.

Hertzberg, R.W., *Deformation and Fracture Mechanics of Engineering Materials*, John Wiley and Sons, Inc., 1989.

Irving, R.R., "The Strength in HSLA is the Microalloying," *Iron Age*, November 1987.

Kiessling, R., *Non-metallic Inclusion In Steel*, The Institute of Metals, London, 1989.

Kiessling, R. and Lange, N., *Nonmetallic Inclusions In Steel*, The Metals Society, London, 1987.

Kou, S., *Welding Metallurgy*, John Wiley and Sons, Inc.,. 1987.

Levin, E.H., Robbins, C.R. and McMurdie, H.F., *Phase Diagrams For Ceramists*, The American Ceramic Society, Inc.,. 1964.

McHale, P.F., *Factors Influencing The Microstructural And Mechanical Properties of ULCB Steel Weldments,* Master's Thesis, Naval Postgraduate School, Monterey, California, December 1991.

Pickering, F.B., *Physical Metallurgy and the Design of Steels*, Applied Science Publishers, 1978.

Ricks, R.A., Howell, P.P. and Barritte, G.S., "The Nature Of Acicular Ferrite In HSLA Steel Weld Metals," *Journal of Materials Science*, v.17,1982.

Samuels, L.E., *Optical Microscopy of Carbon Steels*, American Society for Metals, 1980.

INITIAL DISTRIBUTION LIST

1.	Defense Technical Information Center Cameron Station Alexandria, VA 22304-6145	2
2.	Library, Code 52 Naval Postgraduate School Monterey, CA 93943-5000	2
3.	Department Chairman, Code ME/Kk Department of Mechanical Engineering Naval Postgraduate School Monterey, CA 93943-5000	1
4.	Weapons Engineering Curricular Office, Code 33 Naval Postgraduate School Monterey, CA 93943-5000	1
5.	Professor A.G. Fox, Code ME/Fx Department of Mechanical Engineering Naval Postgraduate School Monterey, CA 93943-5000	2
6.	Dr. M.G. Vassilaros, Code 2814 Naval Surface Warfare Center Annapolis, MD 21402	1
7.	Lt Eugene P. McDonald, USN 10745 Victoria Ave. Whittier, CA 90604	3